IEEE 2012 GLOBECOM
GLOBAL COMMUNICATIONS CONFERENCE, EXHIBITION & INDUSTRY FORUM

Issue 2
Tuesday, 4 December 2012

Tutorials and Workshops kick off IEEE GLOBECOM 2012

Welcome to IEEE GLOBECOM 2012

and this year's schedule consisting of approximately 1,500 keynotes, business panels, industry forums and technical sessions. The conference initiated its premier international agenda with the first of more than 30 workshops and tutorials dedicated to topics ranging from digital gaming and small cell wireless networks to LTE and beyond 4G emerging technologies. Included in these efforts were the presentations of global communications experts representing scores of countries.

Among Monday's 11 workshops was the first-half of the session on "Cloud Base-station and Large-scale Cooperative Communications," which began with the introductory keynote of Dr. Jesse Fang of Intel Corp. on "Challenges & Opportunities in the Age of Mobile Internet." During his presentation, Dr. Fang spoke extensively about the cloud's role in developing future basic station architectures that focus on the fulfillment of user experiences as a measure of success. This included emphasizing the use of ICT technologies for data distribution and improving the mobile network itself to overcome problems like poor user plane services and core network congestion. Other recommendations entailed the building of ecosystems supporting billions of subscribers through the drive for enhanced standardization and policy making.

Shortly afterwards were also several tutorials that included the well-attended sessions on "Digital Games for People Networking – Challenges & Opportunities" and "Small Cell & Heterogeneous Network (HetNet) Deployment." In the session on "Gaming," Ross Smith of Microsoft spoke about "gamification" and the effort to integrate game features into work environments as a method for developing organizational trust, facilitating interactions, breaking cultural barriers and introducing fun into the creative aspects of work. He also highlighted the "magic circle of play" and its ability to support risk taking and experimentation among employees, who are already working well beyond the regular hours of business. Among these individuals are the nearly 70 million individuals in the U.S., who classify themselves as social gamers and the average 18 – 24 year old, who is sending and receiving 100 or more texts a day.

Highlights of the HetNet industry tutorial included an explanation of the Ranplan Radio Propagation Simulator used for modeling an entire campus, indoor and outdoor, within different types of environments ranging from residential areas to stadiums and airports. Described as one of the most powerful tools of its kind for creating superior 3D building models, the Ranplan optimization tool was also featured as an intelligent method for supporting the real-time collection and measurement of data as well as the improved performance of indoor cells.

Programming for the first day of IEEE GLOBECOM 2012 concluded with the second half of the morning's workshops and three more industry forums on "Programmable Cloud Computing," "Internet as a New Paradigm," and "Software Testing in the Network Environment."

PAPER SMART CONFERENCE

IEEE GLOBECOM 2012 is a paper smart conference.
There will be no printed final programs distributed onsite at the conference.
The final program is available at **http://www.ieee-globecom.org/2012/finalprogram.html** in PDF and FlipBook searchable formats.

The conference venues, Disneyland® Hotel and Grand Californian Hotel, will both be equipped with wireless access points. There will also be computer stations available in the registration and exhibit hall areas for thosewho may need to view the conference program.

The only printed material is the Program Guide found in your badge holder.

TABLE OF CONTENTS

PROGRAM SPOTLIGHT

Opening & Keynote Session

Tuesday, 4 December 2012 • 08:00 – 09:30

Henry Samueli

Co-Founder, Chairman & CTO
Broadcom Corporation

Connecting Everything: Dream Becomes Reality

Twenty years ago Broadcom's tagline, 'Connecting everything' was just a dream, but thanks to dramatic advances in technology, that dream has now become reality. The semiconductor industry is the primary technology enabler for this connected universe, demonstrating profound and sustained impact on the entire equipment and services value chain. Our insatiable thirst for rich multimedia content is driving explosive demand for bandwidth over our global communications networks. From broadband access networks to the home, to corporate enterprise networks, to global infrastructure networks, we are seeing capabilities improve by leaps and bounds. Today we also recognize that mobility is central; our smart devices are always on and always with us, perform non-stop, and are expected to adapt to the context and locations in which we are using them. This talk will cover some historical perspectives on how communications technology has evolved to where it is today; will review the current state-of-the-art, and will also give some conjectures on where it might take us in the future.

IF7: Executive Forum: New Technologies to Watch

Tuesday, 4 December 2012
10:00 – 12:00

It is easy to see that the communication industry continues to evolve and change. New technologies, novel processes and innovative tools make bandwidth broader, production easier, cost lower and friendlier to end-users. This session is aimed to look at the future and impact of new communication technologies.

During the panel, the executives will explore various emerging technologies and address questions important to the future of our communication industry.

Invited Guest Speakers:

Glenn Wellbrock, Director, Optical Transport Network -Architecture, Design & Planning, Verizon, USA
Emerging Technologies That Will Shape Our Future

Chen Chang, Founder & CEO, BeeCube, USA
So Many Users, So Many Opportunities, So Little Spectrum, So Little Time

Patrick Diamond, Founder, Patrick Diamond Consulting, USA
Techniques for Precise Time Transfer over Optical Networks

Yong Kwan Park, CEO & President, OE Solutions, Korea
Intelligent Optical Transceivers for Efficient Telecom Network Operation

Dean Sirovica, VP, Business Development, Huawai Technologies, China (Keynote)
New Technologies & their Impact

Glenn Wellbrock

Chen Chang

Patrick Diamond

Yong Kwan Park

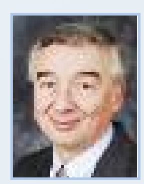

Dean Sirovica

PROGRAM SPOTLIGHT

IF15: Dialogue with Industry Leaders

Tuesday, 4 December 2012
19:00 – 20:30

Sponsored by General Photonics — Making Light Work Lighter

Chairs: Hamid Ahmadi, VP & Head, Advanced System Engineering Lab, Samsung Information Technology America, USA
Glenn Wellbrock, Director, Optical Transport Network -Architecture, Design & Planning, Verizon, USA

This roundtable will provide an excellent opportunity for attendees to participate in cutting-edge discussions and unmatched peer-to-peer networking as they hear real world solutions from various industry leaders that will help better manage their business.

Panelists:
Joe Berthold, VP, Network Architecture, CIENA Corporation, USA
Dean Sirovica, VP, Business Development, Huawai Technologies, USA
Yong Kwan Park, CEO & President, OE Solutions, Korea
Pat Diamond, Founder, Patrick Diamond Consulting, USA
Geoffrey Mattson, VP Architecture, Platform Systems Division CTO, Juniper Networks, USA
Flavio Bonomi, VP & Head, Advanced Architecture and Research Organization, Cisco Systems, USA
Steve Gray, CTO, CSR, USA
Mahbubul Alam, Head of M2M/IoTs, ITS Infrastructure and Auto Manufacturing Connected Industries Group, Cisco, USA


Hamid Ahmadi

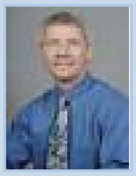
Glenn Wellbrock


Joe Berthold


Dean Sirovica


Yong Kwan Park


Pat Diamond


Geoffrey Mattson


Flavio Bonomi

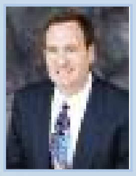
Steve Gray


Mahbubul Alam

IF23: Lightning Talks Session

Thursday, 6 December 2012 • 16:00 – 18:00
North Ballroom A

New to IEEE GLOBECOM!

A lightning talk session is concluding the Industry Forums portion of the conference. ***Lightning talks are short five minute talks on technical topics.*** Any conference related subject can be presented (thoughts triggered by a presentation, a nifty algorithm trick, a thesis project, open source software project, company product, etc.). From 20 to 24 talks will be presented in this 120 minute session.

Rules:
1. ***Sign up at conference registration before Thursday at noon.*** Speaking slots assigned in order of sign up.
2. Speakers must be present at start of session or slot is forfeited to the next speaker signed up.
3. Each speaker is permitted five minutes to speak
a. Use from zero to three slides.
b. Please no animation on the slides.
c. Use of URLs within the presentations is encouraged.
4. The five minute time limit on talks will be strictly enforced. Speakers should be prepared to present a concise talk.
5. Email slides to ***reder@ieee.org*** following the session, if you desire them to be posted on the conference web site.

Turns in-building network design into an engineering art

Professionalism Efficiency Communication Service

RANPLAN produces the world leading RAN planning and optimisation tools – iBuildNet®, Ranplan Radiowave Propagation Simulator (RRPS®), Ranplan-Fi® and Ranplan-HetNet® Suite.

EVENTS OF THE DAY

08:00 – 09:30
OPENING & KEYNOTE SESSION
Henry Samueli, Broadcom
Center Ballroom/North Ballroom A/B

09:30 – 10:00
COFFEE BREAK / South Exhibit Hall
Prize Drawing (must be present to win)

10:00 – 12:00
INDUSTRY FORUMS
IF7: Executive Forum: New Technologies to Watch / South Ballroom A
IF8: M2M/IoT: What are the Futures in Communication? / North Ballroom A

TECHNICAL SESSIONS
AHSN01: Ad Hoc Routing / North Exhibit Hall A
AHSN10: VANETs I / North Exhibit Hall B
CISS01: Social Network Security / North Exhibit Hall C
CogRN01: CRN Applications & Implementation / North Exhibit Hall D
CQ01: Energy Saving in Communication Networks & Equipment / Magic Kingdom Ballroom 4
CSSM01: Multimedia Quality of Service / North Exhibit Hall G
CT01: Theoretical Aspects of Communication Systems / North Exhibit Hall H
NGNI01: Data Centers & Cloud Computing / North Exhibit Hall J
ONS01: Physical Layer Issues & Technologies / Castle A
SAC-GNCS1: Green Systems, Designs and Applications / Castle B
SPC01: MIMO I / Monorail A
SPC02: Compressed Sensing / Monorail B
WC01: Resource Allocation / Monorail C
WC02: Modulation & Coding I / Magic Kingdom Ballroom 1
WC03: UWB I / Castle C
WN01: Femto-cell Networks / North Exhibit Hall I
WN02: Smart Grid Communications / North Exhibit Hall F

12:00 – 13:45
AWARDS LUNCHEON / Center Ballroom

13:45 – 15:30
INDUSTRY FORUMS
IF9: Disruption Tolerant Networks / South Ballroom A
IF10: Smart Enterprise: Next Generation Internet / North Exhibit Hall E
IF11: Green Communication & Computing / North Ballroom A

TECHNICAL SESSIONS
AHSN02: Data Mules & Mobile Sinks / North Exhibit Hall A
AHSN11: Network Coding / North Exhibit Hall B
CISS02: Security in Cloud Computing & Storage / North Exhibit Hall C
CogRN02: Energy Management of Cognitive Radio Networks / North Exhibit Hall D
CQ02: Network Layer Modeling & Design / North Exhibit Hall F
CSSM02: Multimedia Quality of Experience / North Exhibit Hall G
CT08: Cognitive Radio / North Exhibit Hall H
NGNI02: Router Architecture & Switch Design / North Exhibit Hall I
ONS03: Optical Spectrum Management / North Exhibit Hall J
SAC-ASN1: DSL, RoF & Misc. / Castle A
SAC-GNCS2: Green Hardware & Chip Designs / Castle B
SPC03: Relay / Castle C
WC04: Cooperative Communications I / Monorail A
WC05: Heterogeneous Network / Monorail B
WC06: UWB II / Monorail C
WN03: Cellular Networks I / Magic Kingdom Ballroom 1
WN04: 802.11 Wireless Networks / Magic Kingdom Ballroom 4

15:30 – 16:00
COFFEE BREAK / South Exhibit Hall
Prize Drawing (must be present to win)

16:00 – 18:00
INDUSTRY FORUMS
IF12: Social Networks: Impact on Quality of Life / South Ballroom A
IF13: Future Networks, IPv6 Deployment: World Views / North Exhibit Hall E
IF14: The Grand Debate: Internet vs. Telecommunications / North Ballroom A

TECHNICAL SESSIONS
AHSN03: Wireless Sensor Network Routing I / North Exhibit Hall A
AHSN12: VANETs II / North Exhibit Hall B
CISS03: Physical Security / North Exhibit Hall C
CogRN03: Resource Allocation / North Exhibit Hall D
CogRN09: Spectrum Sharing / Magic Kingdom Ballroom 4
CQ03: Cloud Computing & Communication Technology North Exhibit Hall F
CSSM03: Peer-to-Peer Service / North Exhibit Hall H
CT02: Pilot Design & Channel Estimation / North Exhibit Hall I
NGNI03: Mobile & Wireless Networks / North Exhibit Hall J
SAC-GNCS3: Green Wireline Communications / Castle B
SAC-PL 1: Power Line Communications & Smart Grid I / Castle A
SPC04: OFDM & Multicarrier Systems / Castle C
WC07: Cooperative Communications II / Monorail A
WC08: Modulation & Coding II / Monorail B
WC09: Interference Management I / Monorail C
WN05: Handover & Mobility Management / Magic Kingdom Ballroom 1
WN06: Delay Tolerant Networks / North Exhibit Hall G

19:00 – 20:30
DIALOGUE WITH INDUSTRY LEADERS / South Exhibit Hall

PROGRAM UPDATES

The following are updates to the program guide found in your badge holder. These updates appear in the online final program.

Tuesday, 4 December 2012
IF8: M2M/IoT: What are the Futures in Communication?
from 10:00 – 12:00 will now be held in North Ballroom A.
IF11: Green Communication & Computing
from 13:45 – 15:30 will now be held in North Ballroom A.
IF14: The Grand Debate: Internet vs. Telecommunications
from 16:00 – 18:00 will now be held in North Ballroom A.

Wednesday, 5 December 2012
IF17: Next Generation Cellular & Satellite Communication I
from 10:00 – 12:00 will now be held in North Ballroom A.
IF18: Next Generation Cellular & Satellite Communication II
from 13:30 – 15:30 will now be held in North Ballroom A.
IF22: Education Forum
from 16:00 – 18:00 will now be held in North Ballroom A.

Thursday, 6 December 2012
IF25: Cable Industry Access Technology
from 16:00 – 18:00 will now be held in North Ballroom A.
IF28: Optical Wireless Access
from 13:30 – 15:30 will now be held in North Ballroom A.
IF23: Lightning Talks
from 16:00 – 18:00 will now be held in North Ballroom A.

Friday, 7 December 2012
T9: Opportunistic Communication
from 09:00 – 12:00 will now be held in Magic Kingdom Ballroom 1/4.
T12: Cooperative Spectrum Sensing
from 14:00 – 17:00 will now be held in Magic Kingdom Ballroom 1/4.

FEATURED ARTICLES

The "Internet of Things" based on IPv6

By **Latif Ladid**, President IPv6 Forum, University of Luxembourg

Introduction

The public IPv4 address space managed by IANA (http://www.iana.org) has been completely depleted by Feb 1st, 2011. This creates by itself an interesting challenge when adding new things and enabling new services on the Internet. Without public IP addresses, the Internet of Things capabilities would greatly be reduced. Most discussions about IoT have been based on the illusionary assumption that the IP address space is an unlimited resource or it's even taken for granted that IP is like oxygen produced for free by nature. Hopefully, the next generation of Internet Protocol, also known as IPv6 brings a solution.

In early 90s, IPv6 was designed by the IETF IPng (Next Generation) Working Group and promoted by the IPv6 Forum since 1999. Expanding the IPv4 protocol suite with larger address space and defining new capabilities restoring end to end connectivity, and end to end services, several IETF working groups have worked on many deployment scenarios with transition models to interact with IPv4 infrastructure and services. They have also enhanced a combination of features that were not tightly designed or scalable in IPv4 like IP mobility, ad hoc services; etc catering the extreme scenario where IP becomes a commodity service enabling lowest cost networking deployment of large scale sensor networks, RFID, IP in the car, to any imaginable scenario where networking adds value to commodity.

With the exception of very few IPv6 experts, none of the previous discussions or research papers talked explicitly about the IPv4 address crunch and its impact on IoT or the open standards needed for its scalability, let alone ever mentioning IPv6 and its advanced IETF developments such as IPv6 adaptation layer over IEEE 802.15.4 (including header compression) known as 6LoWPAN or IPv6 Routing Protocol for Low power and Lossy Networks (RPL) as the way forward. This paper wishes to restore some sanity in this area.

Open and Scalable Architectural Model

When embedding networking capabilities in "things", there are architectural decisions to be made that guarantees the "Internet of Things" is scalable, inclusive of several communication media, secure, future proof and viable for businesses and end-users. Several models can be discussed, (as reviewed below) but one clearly emerges as the best approach.

1. Closed or monolithic architectures

Today, when studying market segments already integrating networking capabilities in "things", one finds many ad-hoc alliances, proprietary, monolithic or closed protocols. Most of these focus only on the lower layers (Physical and Datalink) of the OSI model to transmit data or else define a complete network stack including application layers that only work on a single communication medium. Fortunately (or unfortunately), it was demonstrated long ago that the Earth is not flat, meaning in our context that a truly scalable network needs more than a single physical and data link layer to fit all of the needs and requirements of a diverse set of applications and use cases.

- A proprietary or monolithic protocol installation requires the upgrade of all networking components when moving to new technologies
- Markets remain fragmented with no interoperability unless done on the obvious protocol of choice-- the Internet Protocol or IP.
- Mix & match of proprietary protocols are costly and inefficient, requiring protocol translation gateways for each protocol stack. Once again, it calls for translation to IP, but use of protocol translation gateways has been proven to be difficult to operate, manage and scale.

Continued next page >>

2. Why not a new protocol suite?
As the "Internet of Things" clearly represents a new generation of devices and applications, some people may think it would be better to begin from scratch and create a new architectural model. Although this may look attractive at first glance, such a proposal has a number of known issues:
- The "Internet of Things" is going to involve not only interactions between things, but also interaction between humans and their computers or their personal devices, as in the case with remote monitoring or remote control applications. By developing an "Internet of Things" separate from the actual Internet it will encourage market fragmentations as well as a "Balkanization" between both the existing Internet and "Internet of Things" in contrast to the convergence to IP that is now happening in areas such as telephony and TV.

- In addition, open standards are key to the success of any protocol. It generally takes between 5 and 10 years from inception to production implementations. An entirely new architecture will delay the "Internet of Things" and be an obstacle to rapid market adoption.

3. The Internet Protocol (IP)
Although certainly not 100% perfect, expecting researchers and others to enhance the protocol suite, the TCP/IP model has demonstrated:
- Capacity to be deployed on a very large scale, aka "The Internet"
- Centralized (i.e.: an Intranet) or distributed (i.e.: The Internet) deployment models
- Versatility to handle all types of traffic, including critical traffic such as voice and video.
- Extensive interoperability as IP runs over most if not all available industry standard network links – wireless (802.15.4/6LoWPAN, Wi-Fi, 3G, WiMax,…) and wired (Ethernet, Sonet/SDH, serial,…).
- Open process of standardizations through the IETF and associated standard bodies, enabling consensus on enhancements and interoperability.
- Future proofing through the adoption of a next generation of IP protocol, aka IPv6.
- Established application level data model and services which are well understood by software developers and widely known to the public through worldwide web applications. The diversity of applications with the web services paradigm is a prominent one thanks to its enablement of distributed computing across platforms, operating systems, programming languages, and of course vendors and products.
- Established network services and architectures for higher-level services and scalable deployments:
    - Naming, addressing, translation, routing, services discovery, load balancing, caching, and mobility.
    - Diversity of well understood security mechanisms at different layers and different scopes.
    - Diversity of network management tools and applications.

Internet Protocol Version
Once it is agreed that IP is the appropriate architectural model, comes the question of recommending an IP version. The Internet today is going through a transition due to the IPv4 address space exhaustion [OECD, IPv4add-report]. With little existing legacy in the "Internet of Things", there is an opportunity to promote IP version 6 (IPv6) as the de-facto IP version for the "Internet of Things". This recommendation would be fully aligned, such as:
- U.S. OMB and FAR
- European Commission IPv6 recommendations
- Regional Internet Registry recommendations
- IPv4 address depletion countdown

Adoption of IPv6 for the "Internet of Things" benefits from:
- A huge address space accommodating any expected multi-millions of deployed "things".
- "Plug & Play" capabilities as IPv6 protocol suite enhance provisioning mechanisms suitable to "Things". Flexibility of address configuration as demonstrated by
    - Stateless IPv6 address configuration
    - DHCP Individual address configuration
    - DHCPv6 Prefix Delegation + Stateless IPv6 configuration
- IPv6 is the future IP addressing standard: De facto IP version supported by new physical and data link layers such as IEEE 802.15.4 and IEEE P1901.2 through the standardized IP adaptation layer – IETF 6LoWPAN WG – which only defines IPv6 as protocol version. No IPv4 standard equivalent has been specified.
- De facto IP version for the standardized IETF Routing Protocol for Low Power and Lossy Networks (RPL) – IETF RoLL WG – as it is an IPv6-only protocol.
- If needed, IPv6 over IPv4 tunnelling or IPv6-IPv4 translation could be achieved when "things" would need to communicate with legacy back-end systems not supporting IPv6. It should be noted that all recent operating systems do support the new IP protocol version [OS], making the "translation" requirement as the least preferable solution.

However, an IPv6 address is not a unique identifier and should not be considered to identify a "thing" as the address is expected to change when that "thing" gets connected in a different location or network.

Security and Privacy
By adopting the TCP/IP architecture for the "Internet of Things", all the lessons from years spent to secure private and public IP infrastructures will apply to the new environments. However, some may consider the "Internet" concept as unsecured or lacking privacy. For this reason, it is important to remind people that security and privacy are a multi-faceted challenge.
- Security of "things"

Continued next page >>

As for any device attached to a network, security represents a multi-layered challenge to get addressed by owners or network managers. It ranges from

- Securing the physical access to a "thing".
- Authenticating the data link, network and application access.
- Encrypting data on data links and network links when necessary – in accordance with regulations.

All existing mechanisms today require appropriate documentation and enhancements for true plug & play.

• Network security

Connecting "things" to an IP environment means all network design and policy already defined in an intranet or when providing access the Internet will apply to the additional sub-networks hosting those "things". It means that at day one, authentication, access control, firewall and intrusion detection mechanisms should fully be operational for the "Internet of Things".

• Privacy

The "Internet of Things" is no more than an additional layer of devices connecting to the Internet. The fact that "things" implement an IP stack does not mean they have to be fully reachable over the Internet. As for any node, it is the responsibility of the owner or network manager to decide if the "things" fully participate in the Internet or stays isolated on an intranet.

In addition, when "things" are fully reachable over the Internet, it is still important to decide who can communicate with them, including new mechanisms where "things" could share a physical network, but be managed and accessed by dedicated entities. Once again, similar mechanisms and policies already set-up for intranet and Internet accesses apply. However, additional standards may be required to see new business model and usage benefiting from the "Internet of Things". For example, imagine smart meters for electricity, gas and water sharing the same end-user's broadband connection. It certainly does not mean that all entities want to share data related to their business between each other. At the same time, they may want to allow access by the "end-user's things" to some of the information capture by the smart meters allowing local actions to be taken for energy savings. This would require new standards efforts to create such models. For example, Zigbee/IP selected an IPv6 (6LoWPAN/RPL) stack for its Smart Energy Profile 2.0

Applications & Services

A successful adoption of the "Internet of Things" will be largely dependent of the availability of applications and services. Similarly to the actual Internet, traffic flows are expected to range from:

• "Things" to back-end servers
• "Things" to end-user's browsers
• "Things" to "things"

Ease of use is a key criteria to address mass market. It cannot be expected that an average end-user would manually enter IP(v6) addresses when installing new "things" on a network. Likewise, it may not be assumed that "things" can permanently store all addresses of other "things" in a network. For those reasons, it is believed there is a strong need to develop and standardize naming services for the "Internet of Things." However, considering the range of traffic flow, naming services must accept address/name resolution for all kind of communications as previously listed. It cannot be envisaged that an "Internet of Things" naming services would be established disconnected from the existing DNS.

Today, the success of the Internet is largely due to the adoption of worldwide web tools, the new generation of collaborative tools or web 2.0 now representing the next step. It is expected that standard web services will be widely implemented by the first generation of applications on the "Internet of Things", especially for management, data presentation and analysis. Some applications may not be web-oriented per se, but would enable communications between two "things," satisfied with a given definition at the application layer.

In some application domains, do exist applications layers that describe device profiles and capabilities in an optimized fashion for low-resource environments. Often times, they are specific to certain devices and interaction types (control-oriented apps like lighting and temperature setting). The IETF CoRE WG and Extended XML (EXI) are examples of enabling such highly optimized and very descriptive application layers to run on any IP device, including those that are resource-constrained – where 6LoWPAN may be used to provide the underlying IP connectivity – as well as those that have more traditional resource footprints like computers, handhelds, and servers.

Conclusion

Definition and adoption of standards-compliant IPv6 stack and standards-compliant Web Services are the key enablers for a "thing" to be effectively operated and managed in the broader "Internet of Things."

References

[1] The Internet Assigned Numbers Authority (IANA), http://www.iana.org
[1] Executive Office of the President, Office of Management and Budget, "Memorandum for the chief information officers", Washington D.C., August 2, 2005, http://www.whitehouse.gov/sites/default/files/omb/assets/omb/memoranda/fy2005/m05-22.pdf
[2] Department of Defense, General Services Administration, National Aeronautics and Space Administration, "Federal Acquisition Regulation; FAR Case 2005-041, Internet Protocol Version 6 (IPv6)", Volume 74, Nmb 236, pp 65605-65607, December 10, 2009, http://edocket.access.gpo.gov/2009/E9-28931.htm
[3] European Commission IPv6 recommendations, http://ec.europa.eu/information_society/policy/ipv6/index_en.htm
[4] American Registry for Internet Numbers (ARIN), "IPv4/IPv5: The Bottom Line", https://www.arin.net/knowledge/v4-v6.html
[5] The IPv4 Depletion Site, http://www.ipv4depletion.com/?page_id=147

Green Communications and Computing: Questions, Reasons, Issues, Challenges, Approaches, and Trends

By **Jinsong Wu**, Bell Laboratories, Shanghai

Recently, the topics on green communications and computing have received many attentions from both industrial and academic researchers. Generally, the importance of green topics comes from globally environmental concerns, including the concerns of not only energy issues but also resource issues. The urgent needs and challenges of resource-sustainable and/or energy-efficient green communications and computing are the results of two simultaneously increasing trends of energy/resource costs and communications bandwidths impacting ecological and economic activities around the world. Substantial reduction of energy and resource consumption in the information & communications technology sectors is expected to be achieved through the innovative use of new architectures, protocols, and algorithms, which may fundamentally change concepts, structures, and designs of conventional communication and computing systems. Research in green communications and computing is inter-disciplinary in nature, since the motivation is to obtain energy and resource efficiencies from various areas and levels of communication infrastructures and systems, and the complex communication systems that are a large-scale network composed of a number of interdependent and independent wired or wireless nodes. As the dedicated organizational support in the IEEE Communications Society, the Technical Subcommittee on Green Communications and Computing (TSCGCC) was established (**http://www.comsoc.org/about/committees/emerging#gcc, https://sites.google.com/site/gcccomsoc/**) in December 2011. The TSCGCC has established four Special Interest Groups (**https://sites.google.com/site/gcccomsoc/sig**), including SIG on Green Cellular Networks, SIG on Green Smart Grid Communications, SIG on Green Data Center and Cloud Computing, and SIG on Green Cognitive Communications and Computing Networks. As one of the online community supports, the TSCGCC also has created LinkedIn IEEE Green Communications and Computing (GCC) Group (**http://www.linkedin.com/groups?gid=4233179**), which currently includes 7 subgroups:

Green Smart Grid Communications (**http://www.linkedin.com/groups?gid=4673294**),
Green Cognitive Communications and Computing (**http://www.linkedin.com/groups?gid=4673298**),
Green Data Center and Cloud Computing (**http://www.linkedin.com/groups?gid=4710147**),
Energy Harvesting (**http://www.linkedin.com/groups?gid=4673300**),
Cloud RAN (Radio Access Network) (**http://www.linkedin.com/groups?gid=4673292**),
Green Wireline Communications and Networking
(**http://www.linkedin.com/groups?gid=4726456**),
and Green Standardizations(**http://www.linkedin.com/groups?gid=4726224**).

As the continuing efforts of Green Panels in IEEE ICC 2012 (**http://www.ieee-icc.org/2012/program/indforums/wed_1615.html**) and IEEE INFOCOM 2012 (**http://www.ieee-infocom.org/2012/panels.html**), we continue our promotion efforts on green topics in IEEE GLOBECOM 2012 Green Communication & Computing Forum (**http://www.ieee-globecom.org/2012/indforum1.html**), where there are several leading experts in the promising and important topics on Green Communication & Computing, who would discuss a number of paradigm-shifting topics can be expected, including but not limited to sustainable and/or green network architecture and approaches, sustainable and/or green hardware or chip designs, sustainable and/or green computing, green electricity transmission and distribution systems, green standardizations. The IEEE GLOBECOM 2012 Green Forum may bring the broad and in-depth vision of the emerging areas to the audiences in both industrial and academic perspectives. This Forum would address the relevant research trends, practical needs, issues, open problems and possible solutions on green communications and computing. As one of the leading enthusiastic efforts in promoting the research and development of green communications and computing, it is definitely expected that this forum would be both informative and entertaining the IEEE GLOBECOM 2012 audiences.

I work with friction stir processing.

"My work includes non-destructive evaluation of weld quality using artificial intelligence and signal processing techniques at the Center for Friction Stir Processing."

Advice to girls interested in technology:

"Embrace the difficulties."

Dr. Antonette Logar | Computer Science

I nourish young minds.

Prolific author of technical papers and renown in the field of control systems, Bozenna's contributions to bright minds and her solutions to complex technical problems have garnered many awards.

Advice to girls interested in technology:

"Do what you love to do, follow your passion."

Dr. Bozenna Pasik Duncan | Mathematician, Control Systems Engineer

I live IT.

Kathy is currently Deputy Program Manager for Missile Defense Agency Command, Control, Battle Management & Communications Spiral 8.2 Product Development

Advice to girls interested in technology:

"Stand out and highlight your intelligence."

Kathy Land | Information Technology

I Change the World. I am an Engineer.

I design faster fibers.

"I am a research engineer who designs new optical fibers, elevates their performance, and gives technical advice to support new standards."

Advice to girls interested in technology:

"Engineering jobs are interesting, rewarding, and helpful to humanity."

Yi Sun | Communications Engineer

I know nano.

"One of my first undergraduate research projects was to grow zinc oxide nanowires using a low-temperature solution method. My senior thesis would later be designed around this work."

Advice to girls interested in technology:

"Ask as many questions as possible."

Ashley Mason | Electrical Engineering Student

I love collaboration.

"Every day I get to see how our students and graduates are tackling the world's most pressing problems."

Advice to girls interested in technology:

"If you love engineering, you'll be great."

Leah Jamieson | Computer Science and Electrical Engineer

Read more about women in engineering at
www.ieee.org/women

Poster Series sponsored by the IEEE Life Members Fund and the IEEE Foundation

IEEE Women in Engineering WIE

IEEE Women in Engineering

IEEE WIE is the largest international professional organization dedicated to promoting women engineers and scientists.

Write to us at women@ieee.org

IEEE

EXHIBIT ESSENTIALS

The Exhibit Hall is a hub of activity, with Poster Sessions and refreshment breaks taking place here. The Exhibit Hall provides the perfect place to mix and mingle with colleagues and friends, and to meet your suppliers.

Prize drawings will be held during the morning and afternoon coffee breaks in the Exhibit Hall. Drop your ticket (included in your registration packet) or business card in the ticket tumbler on the stage in the Exhibit Hall. One prize per attendee. Must be present to win.

Check out the monitor in the Exhibit Hall showcasing the #GLOBECOM Twitter Wall, Yammer comments and ComSoc Presidents' Recollections Video, which can also be found at http://www.ieee-globecom.org/presidents/.

Visit the booths and explore an exciting marketplace of services, tools and new technology all designed for your needs.

BEEcube Inc.

Booth Number: 14

BEEcube is the leading provider of All Programmable Equipment for research, development, prototyping and deployment. BEEcube is at the forefront of technology innovation within Telecom and MILCOM with applications like LTE-Advanced Remote Radio Units and Baseband Units, MIMO Wi-Fi, backhaul links in E-band radio, Software Defined Radio, Software Defined Networking, Military WLAN, Synthetic Aperture Radar, and Phased Array Radar.

Cambridge University Press

Booth Number: 18

Cambridge University Press is a leading publisher in telecommunications, producing authoritative books and journals for students, researchers, and practitioners. Visit our booth to see a range of new titles including 'Networked Life: 20 Questions and Answers', by Mung Chang, 'Principles of Cognitive Radio', by Ezio Biglieri et al., 'OFDMA Mobile Broadband Communications', by Junyi Li, Xinzhou Wu, and Rajiv Laroia, and 'Detection and Estimation for Communication and Radar Systems', by Kung Yao, Flavio Lorenzelli, and Chiao-En Chen, and the open access journal, "APSIPA Transactions on Signal and Information Processing."

Ciena

Booth Number: 10

Ciena is the network specialist. We collaborate with customers worldwide to unlock the strategic potential of their networks and fundamentally change the way they perform and compete. Ciena leverages its deep expertise in packet and optical networking and distributed software automation to delivering solutions in alignment with OPn, its approach for building open next-generation networks. We enable a high-scale, programmable infrastructure that can be controlled and adapted by network-level applications, and provide open interfaces to coordinate computing, storage and network resources in a unified, virtualized environment. We routinely post recent news, financial results and other important announcements and information about Ciena on our website, http://www.ciena.com.

General Photonics

Table #2

General Photonics is the leading supplier of timing and polarization products to the telecommunications, photonics and medical imaging markets. General Photonics supplies a full line of components, modules and instruments that manage and measure polarized light, including a complete suite of emulation instruments for testing the polarization performance of coherent detection systems.

IEEE Cloud Computing Initiative

Booth Number: Table # 1

The IEEE Cloud Computing Initiative is a broad based collaborative project sponsored by the IEEE. The initiative is organized across multiple areas that are interdependent. These include big data, conferences, education, publications, standards and a testbed. A web portal serves as a resource that provides news about the initiative's progress, articles from the IEEE Xplore digital library, conferences sponsored by IEEE and other organizations, standards, educational materials, interviews from experts, and other relevant information. Information will be available on the overall initiative.

IEEE GLOBECOM 2013

Booth Number: 21

The 2013 IEEE Global Communications Conference (GLOBECOM) will be held in Atlanta, GA at the Hilton Hotel, in the heart of downtown's finest eating and tourism establishments. Please join us December 9 – 13, 2013 an unforgettable conference experience. IEEE GLOBECOM 2013 will offer cutting edge communications technology symposia, forums, panel discussions, tutorials, workshops, industry exhibits and renowned industry CEOs & CTOs in panel sessions and keynote speeches. And be sure to schedule some time for yourself and your loved ones to experience many of the nearby family-friendly attractions, such as the largest indoor aquarium in the US, numerous museums for art, history, and science (and Coca Cola, of course!), as well as one of the finest restaurant scenes in North America.

IEEE GLOBECOM 2014

Booth Number: 1

Austin is proud to host the IEEE Communications Society's IEEE Global Communications Conference (GLOBECOM) in the heart of Silicon Hills (technology corridor of the Southwest) from December 8 – 12, 2014 at the Austin Hilton Hotel Complex. IEEE GLOBECOM 2014 will offer the latest technology research for the technical community along with an innovative program for industry management and engineers. Austin has a great music scene, nightlife, weather, and the conference will be held right in the heart of the most vibrant downtown in the southern United States, and one of America's fastest growing, youngest, and most desirable cities.

IEEE ICC 2013

Booth Number: 15

IEEE ICC 2013 will be held in the charming city of Budapest, Hungary from June 9 – 13, 2013. The conference will be hosted in three adjacent five-star hotels in the very heart of the city, on the banks of the river Danube. The hotels offer magnificent panoramic views across the river, the Gellert Hill and the Royal Castle District, part of the UNESCO World Heritage. Submissions to the technical symposia have now been closed. However, you can still submit your contribution to 28 topical workshops held in conjunction with the main conference. We much look forward to an enlightening and enjoyable event with you!

EXHIBIT ESSENTIALS

IEEE ICC 2014

Booth Number: 2

The 2014 IEEE International Conference on Communications (ICC) will be held in the beautiful city of Sydney, Australia from June 16 – 20, 2014. Themed "Communications: The Centrepoint of Digital Economy," this flagship conference of IEEE Communications Society will feature a comprehensive technical program including twelve Symposia and a number of Tutorials and Workshops. IEEE ICC 2014 will also include an exceptional expo program including keynote speakers and Industry Forum & Exhibitions.

IEEE ICC 2015

Booth Number: 3

The 2015 IEEE International Conference on Communications (ICC) will be hosted in June 2015 in ExCel London, the largest convention center in the United Kingdom. London is the largest metropolitan area in the United Kingdom and the largest urban zone in the European Union. It is a leading global city, with strengths in the arts, commerce, education, entertainment, fashion, finance, healthcare, media, professional services, research and development, tourism and transport. London has become the first city to host the Summer Olympics three times. For more information, please contact Executive Chairman Professor Jiangzhou Wang of University of Kent at j.z.wang@kent.ac.uk.

IEEE Women in Engineering (WIE)

Booth Number: 16

The mission of IEEE WIE is to facilitate the recruitment and retention of women in technical disciplines globally. IEEE WIE envisions a vibrant community of IEEE women and men collectively using their diverse talents to innovate for the benefit of humanity. Goals include facilitating the development of programs and activities that promote the entry into and retention of women in engineering programs and enhancing the career advancement of women in the profession.

National Instruments

Booth Number: 9

Since 1976, National Instruments has equipped engineers and scientists with tools that accelerate productivity, innovation, and discovery. NI's graphical system design approach to engineering provides an integrated software and hardware platform that speeds the development of any system needing measurement and control. With NI software defined radio (SDR) solutions, engineers can build powerful, flexible systems spanning design to test applications. NI LabVIEW software offers a single platform that abstracts hardware complexities to shorten user learning curves without sacrificing flexibility. The unique integrated flow encompasses heterogeneous multiprocessing, allowing for scalable solutions. NI also delivers a new approach to RF and communications education through affordable SDR solutions by providing opportunities for hands-on implementation and exploration of a working communications system with live signals.

RANPLAN Wireless Network Design Ltd.

Booth Number: 17

RANPLAN Wireless Network Design Ltd. is a wireless technology company that produces the world leading in-building wireless network planning and optimisation (P&O) software tool – iBuildNet®, a world leading radio propagation tool Ranplan Radiowave Propagation Simulator (RRPS), and world leading WiFi and small cell/HetNet optimization tools Ranplan-Fi® and Ranplan-HetNet® Suite. For more information about RANPLAN and the services and products it provides, please visit www.ranplan.co.uk.

Saracen

Booth Number: 8

The SARACEN (Socially Aware, collaboRative, scAlable Coding mEdia distribution) EU project will demonstrate the results of the work performed in multimedia networking, towards the definition and prototype implementation of a platform for streaming media delivery over P2P architectures, featuring social networking capabilities. The demonstration will rely on the exhibition of a working prototype which will be able to stream content over P2P and use a DLNA compatible device to reproduce it in a home environment. In parallel, demonstration of a smart switching between 2D and 3D based on the automatic detection of use (or not) of 3D glasses will be demonstrated.

Finally, in order to demonstrate the social networking capabilities of the platform, IEEE GLOBECOM participants will be invited to participate in a User Generated Content contest in which videos having as topic the conference will be able to be uploaded, commented and tagged through the SARACEN Social Networking API.

Springer

Booth Number: 19

Springer is a leading publisher of books, journals and electronic products. Visit us to purchase our latest publications at a 20% conference discount. Our publishers are available to answer any questions you may have. Visit springer.com/engineering for more information on our latest products.

Wiley-Blackwell

Booth Number: 7

Wiley's Scientific, Technical, Medical, and Scholarly (STMS) business, also known as Wiley-Blackwell, serves the world's research and scholarly communities, and is the largest publisher for professional and scholarly societies. Wiley-Blackwell's programs encompass journals, books, major reference works, databases, and laboratory manuals, offered in print and electronically. Through Wiley Online Library, we provide online access to a broad range of STMS content: over 4 million articles from 1,500 journals, 9,000+ books, and many reference works and databases.

Monday Afternoon Industry Tutorials Detailed New M2M, Cloud Computing & Cognitive Radio Advances

Yesterday afternoon, a full room of attendees participating in the "M2M Smart Grid & Smart Cities" industry tutorial learned of the latest efforts to seamlessly connect billions of subscribers to trillions of objects in real-time, while maximizing energy efficiencies and minimizing the production of harmful hydrocarbons. Described as the "Industrial Internet," Mischa Dohler of the Centre Tecnològic de Telecomunicacions de Catalunya (CTTC) in Spain addressed the ongoing efforts to connect the two worlds of ICT and energy and seamlessly gather cross domains of data that will produce, smarter and cleaner methods for supporting the world's population. This includes the one out of two individuals that live in cities worldwide and the two million people that die annually from pollution-related events.

Highlighted in his discussion was an in-depth introduction to M2M systems, standards compliant low-power multihop networking designs as well as low power Wifi and their combined ability to automate instrumentation capable of monitoring parking, traffic, trash bins and public lighting in an attempt to reduce the manpower and energy accompanying these activities. According to Dohler, the key to this future energy landscape is the development of standards and flat architectures that link the various worlds in this ecosystem, while creating applications that benefit widespread industrial and humanitarian purposes.

Other afternoon sessions on Monday drew hundreds of attendees to the industry tutorials on "Programmable Cloud Computing & Networking," "Wireless Cognitive Radio," "Internet as a New Paradigm and "Software Testing in the Network Environment." In his session highlighting Internet paradigms, Bob Frankston, IEEE Fellow, detailed the principles enabling innovations in connectivity within homes and other venues, while the "Quality of Service Provisioning in Wireless Cognitive Radio Network" presentation addressed scores of participants about the rapid emergence of cognitive radio technologies and the new methods for increasing spectrum efficiency and driving the advance of QoS-assurance wireless cognitive radio networks.

First Day of IEEE GLOBECOM 2012 Concluded with Evening of Fine Dining, Good Company & Entertainment

Hundreds of IEEE GLOBECOM 2012 participants mingled and socialized during Monday night's first-ever, First Time Attendee Reception held at the Sleeping Beauty Pavilion in the Fantasy Tower of the Disneyland Hotel. Leading the welcome to this flagship conference of the IEEE Communications Society was Bruce Worthman, the society's Director, Conferences, Finance & Administration IEEE Communications, who thanked all the new-comers for their attendance, while introducing the evening's speakers.

In addition to the opportunity to meet and greet new and existing friends, IEEE ComSoc President Vijay Bhargava spoke of the first IEEE GLOBCOM he attended in 1972 and cited the society's 60th anniversary as an example of its ongoing dedication to the advance of communications worldwide. Paul Hartmann, IEEE ComSoc's acting GIMS Committee Chair then followed the comments of IEEE ComSoc Vice President of Conferences Abbas Jamalipour by reinforcing IEEE GLOBECOM's global status as a premier venue for watching technologies grow and collaborating with colleagues who deeply share their interests and expertise.

Afterwards, IEEE GLOBECOM 2012 Executive Chair Pierre Perra offered all the attendees the opportunity to experience the wealth of knowledge offered by the hundreds of sessions, tutorial and workshops comprising this year's agenda. He also invited everyone to share their comments with global colleagues, friends and family through the conference's Twitter, Facebook Yammer and LinkedIn sites located at www.ieee-globecom.org/2012.

Immediately following this introductory get-together, IEEE GLOBECOM 2012 attendees filled the South Exhibit Hall of the Disney Hotel's Fantasy Tower for the Annual Welcome Reception & Exhibition Hall Grand Opening. After the welcoming remarks of IEEE ComSoc President Vijay Bhargava and IEEE GLOBECOM 2012 Executive Chair Pierre Perra, participants toured the exhibits of leading companies like Ciena, Ranplan Wireless Net Design, Cambridge University Press and Springer, while dining on roast beef, turkey, sushi, pasta, chicken ravioli and an assortment of chocolate-covered deserts. In the background, Ryan Andreas, the 2011 "America's Got Talent" competitor serenaded the audience with the music of Elton John and numerous other leading singers and composers.

IEEE GLOBECOM 2012
BEST PAPERS

On the following pages, the 3 of 15 papers featured are from Symposia on Communications QoS, Reliability, and Modeling, Signal Processing for Communications and Next Generation Networking and Internet.

A Robust WiMAX Scheduler for EPON-WiMAX Networks

Mariana P. Dias and Nelson L. S. da Fonseca
Institute of Computing, University of Campinas

***Abstract*—The integration of WiMAX networks with EPON networks capitalizes on the large availability of bandwidth in optical access networks with the mobility provided by wireless technologies. In this integration, a WiMAX scheduler needs to take into account the variability of the channel capacity provided by the EPON scheduler. This paper evaluates the performance of the Deficit Based QoS Uplink Scheduler (DBQUS) mechanism, a standard-compliant WiMAX uplink scheduler designed to operate in ONU-BS, under different EPON service cycle durations. The evaluation is conducted using integrated simulators for the WiMAX and for the EPON components. Results show that the proposed scheduler is able to provide QoS to the subscriber stations under different EPON service cycles. As the traffic load increases, the bandwidth received by the BE service flow is reduced due to the service provided to classes of service with higher priority.**

***Index Terms*—WiMAX, EPON, Quality of Service, Scheduling, Integrated Network.**

I. Introduction

The integration of wireless and optical access networks capitalizes on the advantage of large bandwidth availability of optical networks as well as on the mobility provided by wireless networks.

Among the broadband access technologies the Worldwide Interoperability for Microwave Access (WiMAX) [1] and optical Ethernet Passive Optical Network (EPON) [2] technologies have been successfully deployed in several countries and can be easily integrated since the majority of WiMAX Base Stations comes with an ethernet port that can be plugged into Optical Network Unit (ONU). WiMAX is a broadband wireless access network that provides Quality of Service (QoS), wide coverage, low cost infrastructure and high speed access while EPON is an optical access network with no active elements which provides large amount of bandwidth to the users.

These two technologies have several similarities. They can work in point to multipoint infrastructures and they adopt polling bandwidth granting protocol. Both EPON and WiMAX employ a request/grant mechanism for bandwidth allocation.

In EPON, the Optical Line Terminal (OLT) polls the ONU for bandwidth requests while in WiMAX networks the base stations (BS) poll the subscriber stations (SSs).

Different architectures for this integration have been proposed [3]. In the hybrid architecture, the WiMAX base station is a client of the EPON network and it is connected to an ONU of the EPON, denoted as ONU-BS. In the EPON network, the OLT distributes the available bandwidth among the ONUs in a cyclical way, at every round of bandwidth granting, the EPON protocol decides the amount of bandwidth each ONU will receive. In addition, the bandwidth granted to the ONU-BS must be distributed among the SSs.

In such integrated network, the bandwidth received by the BS changes at every round of the EPON bandwidth granting cycle. Therefore, the WiMAX scheduler located at the ONU-BS should take into account this variability when providing transmission opportunities to its SSs. It is possible that the BS receives less bandwidth in a round than the necessary to support the QoS requirements of its connections. Therefore, special WiMAX scheduler needs to be defined for dealing with such variabilities to provide QoS support to its connections. Indeed, the bandwidth granting cycle of these two networks can be different which imposes extra challenges to the QoS provisioning to the WiMAX SSs.

This paper evaluates the DBQUS WiMAX scheduler for integrated EPON-WiMAX [4] networks, a standard compliant scheduler, in scenarios in which there are differences between bandwidth cycles duration. Most of existing work [5] [6] [7] [8] [9] [10] proposes changes or even new bandwidth granting protocols for the EPON part of the integrated network. Conversely, the DBQUS scheduler has the great advantage of being independent of the EPON protocol adopted. This facilitates the deployment of EPON-WiMAX networks since no change is needed in the EPON network. Results derived via simulation show that the new DBQUS scheduler is capable to provide the QoS requirements of the WiMAX connections as well it is robust to the differences between bandwidth granting cycle duration of these two networks.

This paper is organized as follows. Section II shows related work. Section III describes the integrated EPON-WiMAX network design and operation. Section IV presents the DBQUS scheduling mechanism. Section V gives details on how the simulation experiments were conducted. Section VI shows the analysis of the results obtained. Section VII draws conclusions.

II. Related work

Several scheduling mechanisms have been proposed to integrated EPON-WiMAX networks.

In [5], the authors proposed the QoS-based Dynamic Bandwidth Allocation (QDBA) together with the Prediction-based Fair Excessive Bandwidth Allocation (PFEBA) scheme to enhance the system performance in EPONs. In QDBA, each

ONU handles three queues with different priorities and it also classifies WiMAX traffics into these three priority levels for assigning the traffic to different queues.

The dynamic bandwidth allocation scheme in [6], considered an integrated network to enable data transmission across optical and wireless networks, and an end-to-end differentiated service for diverse QoS requirements. This QoS-aware scheme supports bandwidth fairness at the ONU-BS level and class of service at the WiMAX subscriber station level. The authors had also evaluated the integrated network by examining the effect of EPON service cycle and WiMAX frame duration under different SS numbers.

A QoS-aware scheduling mechanism for the integrated EPON-WiMAX network is proposed in [9] but it does not consider the size of the ONU queues.

In [10], a two-level scheduling scheme for the integrated EPON-WiMAX network was proposed which takes into consideration the queue length and head-of-line (HoL) delays. In this scheme, it is used proportional fairness scheduling for the SSs and a centralized mechanism at OLT that connects to multiple ONU-BSs.

None of these bandwidth allocation mechanisms support all service flows defined in the WiMAX standards. The scheduler proposed here is for the ONU-BS and it has the great advantage of being independent of the EPON protocol adopted. This facilitates the deployment of EPON-WiMAX networks and increases its benefits.

III. EPON-WIMAX INTEGRATED NETWORK

In the considered EPON-WiMAX network [3], the WiMaX BS of is a client of the EPON network and it is connected to an ONU of the EPON (ONU-BS) (Figure 1). In the EPON network, the OLT distributes the available bandwidth among the ONUs in a cyclical way using the Interleaved Pooling with Adaptive Cycle Time (IPACT) [11] protocol. At every round of the bandwidth granting cycle, the EPON protocol decides the amount of bandwidth each ONU will receive. In the IPACT protocol, the OLT polls ONUs and grants time slots to each ONU in a round-robin fashion. The duration of the allocated time slot is determined by the request message sent by the ONUs.

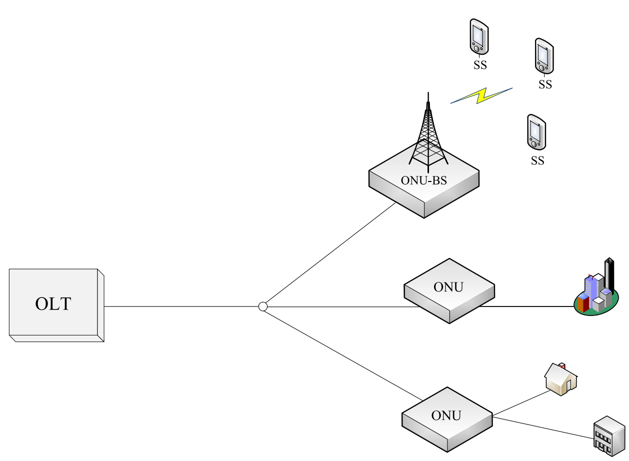

Fig. 1. Integrated architecture of EPON and WiMAX Networks

In addition, the bandwidth granted to the ONU-BS must be distributed among the WiMAX SSs. In such integrated network, the bandwidth received by the BS can change at every round of the EPON bandwidth granting cycle. Therefore, the WiMAX scheduler located at the ONU-BS should take into account this variability when providing transmission opportunities to its SS. It is possible that the BS receives less bandwidth than the necessary to support the QoS requirement of its connections.

The IEEE 802.ah standard specifies that the Multipoint Control Protocol (MPCP) [2] should be used for bandwidth request and granting between the OLT and the ONUs. In the MPCP, the ONUs send report messages to the OLT to solicite the bandwidth needed to transmit their backlog. The OLT sends gate messages to the ONUs to inform their bandwidth grant at every round of the bandwidth granting cycle.

In the WiMAX network, a signaling mechanism for information exchange between the BS and SSs was defined. This signaling mechanism allows the SSs to request bandwidth to the BS. Bandwidth allocation is provided on demand. When an SS has backlogged data, it sends a bandwidth request to the BS. The BS controls the bandwidth allocation to the SSs using the poll/request/grant scheme and allocates time slots to the SSs based on the bandwidth request as well as on the QoS requirements of the requesting connection.

Moreover, the bandwidth granting cycle in the EPON network can be different from that of the WiMAX network which requires that the WiMAX scheduler adjust the bandwidth granted to the SSs so that the QoS requirements of their connections can be supported.

Figure 2 illustrates the workflow of the control messages for bandwidth request and bandwidth grant in the integrated network. The ONU-BS request bandwidth based on MPCP using a REPORT message at each EPON cycle and receives a GATE message for bandwidth grant. The bandwidth granted to the ONU-BS is then distributed to the SSs according to the DBQUS. In the WiMAX network a similar mechanism is used. Each SS requests bandwidth and receives the notification of the the bandwidth allocated by the DBQUS in a cycle.

IV. DBQUS SCHEDULER

This section presents a WiMAX uplink scheduler for EPON-WiMAX networks. The mechanism called, *Deficit based QoS Uplink Scheduler* (DBQUS) [4], is based on the *Migration-based Scheduler for QoS Provisioning* (MBQoS) proposed in [12][13], which does not take into account the variability of channel capacity.

The DBQUS scheduler keeps track of the amount of bandwidth that was not supplied to each connection (*deficitMinimum*) due to bandwidth limitation. Such deficit occurs when the bandwidth given to a connection is below the minimum required. In DBQUS, the deficit is compensated by furnishing additional bandwidth as soon as possible so that the minimum bandwidth requirement is supported. Such compensation is provided to the connections according to a decreasing order of priority.

The proposed scheduler uses three queues, each with a different priority level: low, intermediate and high priority

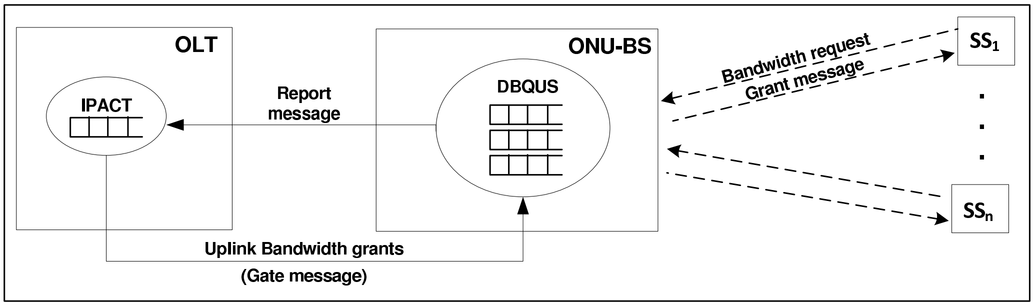

Fig. 2. Workflow of the bandwidth request and grant in the integrated network

queues. The scheduler serves the queues according to their level of priority. The low priority queue stores the BE (Best Effort) bandwidth requests. The intermediate queue stores bandwidth requests sent by both rtPS (real time Polling Service) and nrtPS (non real time Polling Service) connections. These requests can migrate to the high priority queue to guarantee that their QoS requirements are met. In addition to the requests migrating from the intermediate queue, the high priority queue stores periodic grants and unicast request opportunities that must be scheduled in the following frame. UGS (Unsolicited Grant Service) and ertPS (extended real-time PollingService) service flows are served by the high priority queue. The uplink scheduler is executed at every frame, and it broadcasts the scheduling agenda to the SSs in the UL-MAP message. Every time the scheduler is executed, it computes a priority value for each request at the intermediate queue, considering the *deficitMinimum* value of each connection. By doing so, the scheduler tries to compensate the deficits created by the lack of bandwidth. After migrating requests with positive *deficitMinimum*, it computes a priority value for the remaining requests in the intermediate queue, considering the per connection: minimum reserved traffic rate, backlogged requests (number of bytes requested by the connections), and traffic rate received in the current window. Low priority values are assigned to the requests of connections which have already received the minimum reserved traffic rate in the current window. For the remaining requests, the lower the rate received by the connection, the higher is its priority value.

The DBQUS guarantees that the sum of the bandwidth allocated to a single connection is less or equal to the maximum traffic burst requirement. Moreover, the scheduler does not allocate bandwidth for a connection if it results in violation of the maximum sustained traffic rate. As in the MBQoS scheduler [12], a dual leaky bucket is used for maximum burst and maximum rate policing.

The Algorithm DBQUS describes the scheduling scheme. After inserting the periodic grants in the high priority queue, the algorithm checks which rtPS and nrtPS requests should migrate from the intermediate queue to the high priority queue (Lines 2, 3 and 4). In Line 5, the scheduler distributes the available resources among the BE connections if there is no demand from other service flows, and on the final step, the scheduler serves all the requests in the high priority queue, when there is available bandwidth.

The **checkGrants** procedure prioritizes UGS and ertPS connections that have bandwidth deficit. First, it verifies if there is any UGS flow with positive *deficitMinimum*, i.e., if some previous request was not attended. These requests have the highest priority value and they are inserted in the high priority queue while there is available bandwidth for that (Lines 1 to 3). Then, periodic grants for UGS flows that must be served in the next frame are granted (Line 4). After that, this process is repeated for the ertPS flows, prioritizing flows with positive *deficitMinimum* (Lines 5 to 8).

Algorithm 1 DBQUS Algorithm

```
1: checkGrants
2: checkMinimumBandwidth(deficitMinimum)
3: checkDeadline
4: checkMinimumBandwidth(deficit)
5: distributeFreeResources
6: schedule the requests in the high priority queue starting from the
   head of the queue;
```

The **checkMinimumBandwidth** (*deficitMinimum*) tries to meet the bandwidth requirement of rtPS and nrtPS connections with positive *deficitMinimum*. First, it calculates a priority value for each request in the intermediate queue (Line 25). Then, it sorts the intermediate queue by non-decreasing priority values (Line 31). Finally, the scheduler tries to migrate the requests to the high priority queue using the migrateBWRequest procedure according to the requests priority values (Lines 32 to 35).

In the **checkDeadline** procedure, the scheduler tries to migrate rtPS request in the intermediate queue to the high priority queue using the procedure migrateBWRequest in case there is available bandwidth. Requests that are migrated are those with deadline expiring in the frame (Line 14) that follows the next one and those that have not received the minimum reserved traffic rate ($minTR[CID]$) in the current window.

The **checkMinimumBandwidth**(deficit) procedure is similar to the **checkMinimumBandwidth**(*deficitMinimum*) procedure. They differ on how to determine the priority value of a request (Lines 18 and 19). At this point, no request has *deficitMinimum*, so request are sorted by the *deficit* value to obtain the Minimum Reserved Traffic Rate (Line 23).

The **migrateBWRequest** procedure checks whether or not the amount of bandwidth solicited by the request being migrated is available in the uplink subframe. In case the amount of available bandwidth is less than the requested amount, only the available bandwidth will be allocated at

Algorithm 2 Procedures

```
1: checkGrants
2: for each UGS connection u do
3:     if availableBW > 0 and deficitMinimum[u] > 0 then
4:         MigrateBWRequest(u);
5: Insert the UGS grants while availableBW > 0
6: for each ertPS connection e do
7:     if availableBW > 0 and deficitMinimum[e] > 0 then
8:         MigrateBWRequest(e);
9: Insert the ertPS grants while availableBW > 0
10: checkDeadline
11: for each request i at the intermediate queue do
12:     if avilableBW == 0 then
13:         break;
14:     if service[CID] == rtPS then
15:         frame[i] = ⌊(deadline[i] - currentTime) / frameDuration⌋;
16:         if frame[i] == 3 and TwndTR[CID] < minTR[CID] then
17:             MigrateBWRequest(i);
18: checkMinimumBandwidth (priority type)
19: for each connection of type rtPS ou nrtPS do
20:     backlogged_tmp[CID] = backlogged[CID];
21:     TwndTR_tmp[CID] = TwndTR[CID];
22:     bucket2_tmp[CID] = bucket2[CID];
23: for each request i at the intermediate queue do
24:     if minTR[CID] ≤ TwndTR_tmp[CID] or bucket2_tmp[CID]
        == 0 then
25:         priority[i] = 0;
26:     else
27:         if priorityType == deficitMinimum then
28:             priority[i] = backlogged_tmp[CID] -
                (TwndTR_tmp[CID] - minTR[CID]);
29:         else
30:             priority[i] = minTR[CID] - TwndTR_tmp[CID];
31:         TwndTR_tmp[CID] = TwndTR_tmp[CID] + BR[i];
32:         bucket2_tmp[CID] = bucket2_tmp[CID] + BR[i];
33:         backlogged_tmp[CID] = backlogged_tmp[CID] - BR[i];
34: Sort the intermediate queue by priority in non-decreasing order.
35: for each request i at the intermediate queue do
36:     if avilableBW == 0 or (priorityType == deficitMinimum and
        priority[i] ≤ 0 ) then
37:         break;
38:     MigrateBWRequest(i);
39: DistributeFreeResources
40: for each connection of type BE do
41:     if avilableBW = 0 then
42:         break;
43:     MigrateBWRequest(i);
44: MigrateBWRequest(i)
45: if BR[i] > avilableBW then
46:     grantSize = availbleBw;
47: else
48:     grantSize = BR[i];
49: if grantSize > bucket2[CID] then
50:     grantSize = bucket2[CID];
51: if 0 < grantSize < BR[i] then
52:     Create a new request j for connection CID with BR[j] = BR[i]
        - grantSize;
53:     Insert request j in the end of the intermediate queue;
54: BR[i] = grantSize;
55: Move the request i to the high priority queue;
56: TwndTR[CID] = TwndTR[CID] + grantSize;
57: bucket2[CID] = bucket2[CID] - grantSize;
58: backlogged[CID] = backlogged[CID] - grantSize;
59: availableBW = availableBW - grantSize;
```

this scheduling time (Line 43). The allocation of part of the requested bandwidth will be deferred in case it results in violation of the maximum traffic burst requirement. Once the amount of bandwidth that can be allocated to the request is defined (*grantSize*) and if the *grantSize* value is less than the bandwidth requested by a connection, a new request is created with size equal to the amount of bandwidth that will be migrated and, after that, it is inserted at the end of the intermediate queue (Lines 46 to 48). The amount of bandwidth solicited by a request is updated to grantSize and the request is migrated to the high priority queue (Line 50).

The **distributeFreeResources** procedure distributes the available bandwidth, if any, among the BE requests by migrating the chosen requests from the low priority queue to the high priority queue (Lines 36 to 39).

V. Simulation

The effectiveness of the DBQUS was assessed by simulation using the WiMAX module of the Network Simulator (NS-3) [14]. The EPON module was designed in Java. The duration of each simulation was 1200 seconds. Confidence interval with 95% confidence level were derived by the method of independent replication.

The simulated network consisted of 15 ONUs, 1 ONU-BS and a set of 25 SSs. The capacity of the ONU-BS is 30Mbps and the EPON channel is 1Gbps. Each SS has only one service flow. The experiments used different types of traffic: voice, voice with silence suppression, video and FTP, which were associated with UGS, ertPS, rtPS and nrtPS services.

The traffic was generated in the WiMAX network as follows. The voice model used was an exponential on/off model. The mean duration of the on and of the off periods equals to 1.2 s and 1.8 s, respectively. During the on periods, 66-byte packets are generated at every 20-ms. The voice with silence suppression model used the Enhanced Variable Rate Codec (EVRC) [15], with packets generated every 20 ms employing Rate 1 (171 bits/packet), Rate 1/2 (80 bits/packet), Rate 1/4 (40 bits/packet) or Rate 1/8 (16 bits/packet). Video traffic was generated by real video traces [16]. FTP traffic was generated using an exponential distribution with a mean of 512 KBytes.

To generate the ONU's traffic, CBR sources generate 24 byte packets at every 125μs as well as ON-OFF pareto sources. Inter burst generation time is exponential distributed and the burst duration is Pareto distributed and packet lengths were of 594 and 1518 bytes long [17].

The maximum latency requirement for rtPS connections was 300 ms. Each connection had its own minimum reserved traffic rate requirement and maximum sustained traffic rate which varied according to the rate of the transmitted video. The nrtPS service reserved traffic rate requirement and maximum sustained traffic rate requirement are 200Kbps and 800 Kbps, respectively. The unsolicited grant interval requirement for UGS and ertPS was 20ms. The BE service does not have any QoS requirement.

VI. Numerical Results

This section evaluates the robustness of the proposed scheduler via simulation. The aim of these experiments is to assess

TABLE I
SIMULATION PARAMETERS

Number of ONUs	15
Number of ONU-BS	1
Number of SSs	25
WiMAX maximum data rate	30Mbps
EPON maximum data rate	1Gbps
Buffer size in ONU	10Mbyte
WiMAX frame length	5ms
PON cycle time	2ms and 10ms

the DBQUS ability to support QoS requirements of the SSs connections under variable bandwidth furnished by the EPON scheduler. In additional objective is to evaluate the DBQUS capacities of supporting QoS when there is a mismatch between the bandwidth granting cycle of the EPON network and the granting cycle of the WiMAX network.

The simulation scenario includes one ONU-BS and 25 SSs in steps of 5 units (one new SS for each type of service). Table I shows the simulation parameters used in the simulation.

Figures 3 and 4 show, respectively, the throughput and delay per SS as a function of the number of SSs for different values of the EPON cycle duration.

As expected the per station throughput decreases as the number of SSs increases, having a sharper decrease in networks with 20 SSs given the saturation of the network. Moreover, the longer the EPON cycle, the higher is the throughput achieved by the SSs given the reduced overhead for granting the required bandwidth by the SSs.

The delay (Figure 4) increases with the increase of the duration of the EPON cycle since the SSs have to wait longer to receive their bandwidth grant. With 20 SSs, the network is saturated and the delay starts to increase sharply. However, as will be shown in the following figures, the QoS requirements of the connections are supported regardless the aggregated increase of the delay.

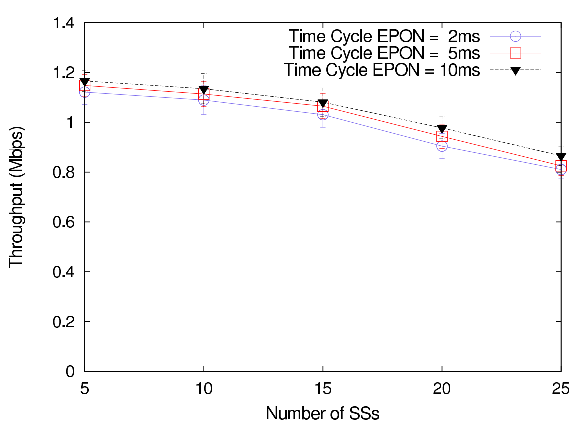

Fig. 3. Throughput of SSs under different EPON cycle time

Figure 5 shows the throughput achieved by UGS, ertPS, nrtPS and rtPS connections for an EPON cycle time of 2ms. The UGS and ertPS throughput did not change, since these classes have high priority which shows that periodic

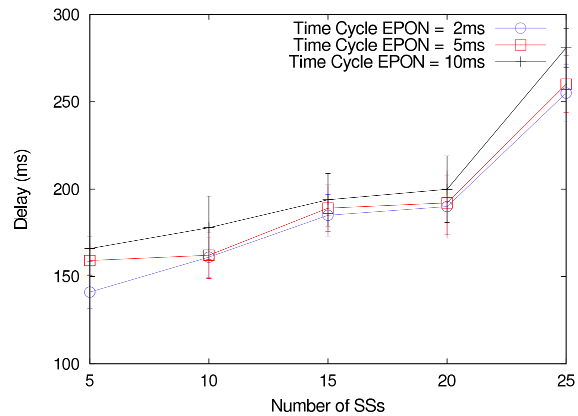

Fig. 4. Delay of SSs under different EPON cycle time

grants are given to them at constant intervals. The nrtPS throughput stayed between the minimum reserved traffic rate requirement (200Kbps) and the maximum reserved traffic rate requirement (800Kbps). As the traffic load increases, the throughput decreases since there are more connections competing for the same resource, nonetheless, the minimum reserved traffic rate requirement is supported. The minimum reserved traffic rate value of 150Kbps for rtPS connections is also supported. Despite the bandwidth variabilities and the number of connections, the throughput requirement are supported.

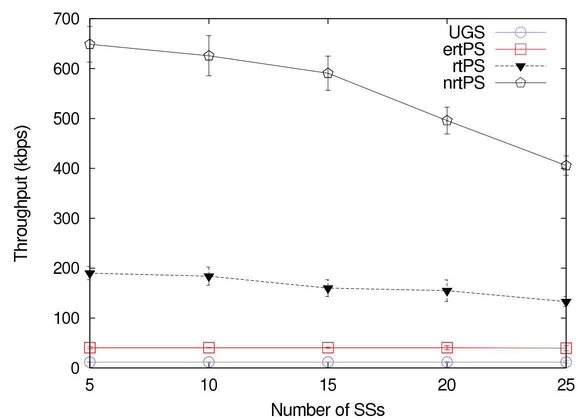

Fig. 5. Average throughput of SSs under 2ms EPON cycle time

Figure 6 shows the latency for the UGS, ertPS and rtPS connections under EPON cycle time of 2ms. The latency of UGS were not affected, even under the variability of channel capacity since these connections have high priority. The latency of ertPS flows were almost constant, but it slightly increases when the traffic load in the network increases. Besides that, the delay values of rtPS connections are below the maximum delay bound of 300ms. The latency of nrtPS flows are not showed in the figure since these connections do not have latency requirements. It is important to note that DBQUS was able to provide delay values below the required bound even when the offered load increased.

For EPON cycle time of 10ms (Figure 7), the throughput of rtPS and nrtPS is higher than those in Figure 5 which was already expected. The DBQUS assured the QoS requirements

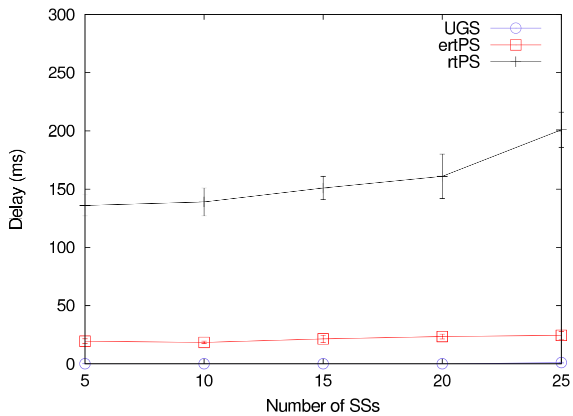

Fig. 6. Average delay of SSs under 2ms EPON cycle time

for UGS, ertPS, rtPS and nrtPS services. In despite of the delay increase (Figure 8), the DBQUS assured the QoS requirements. The latency of UGS slightly increased but the latencies stayed below the bound of its QoS requirement, and for ertPS the trend was the same. For both service classes the latency slightly increased when the traffic load in the network increases. Besides that, the delay values of rtPS connections are still below the maximum delay bound of 300ms.

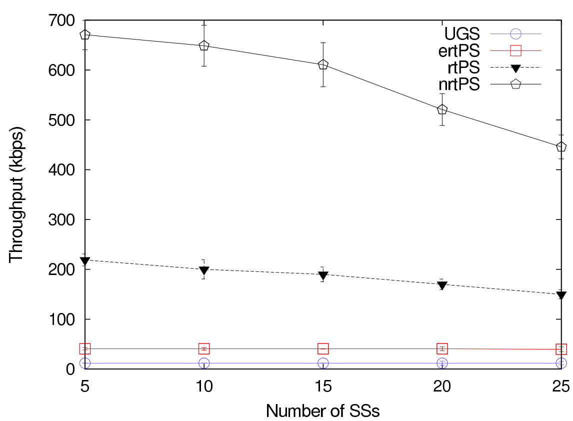

Fig. 7. Average throughput of SSs under 10ms EPON cycle time

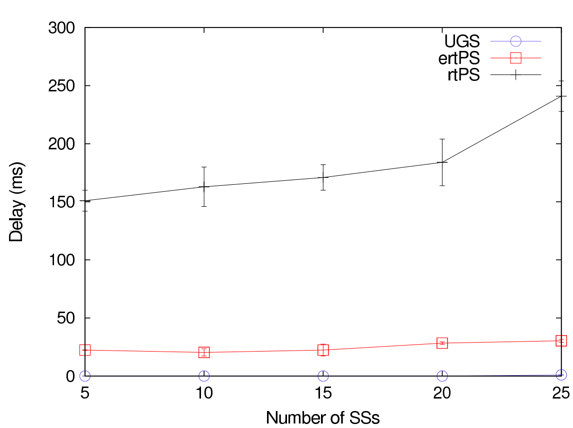

Fig. 8. Average delay of SSs under 10ms EPON cycle time

VII. Conclusions

In this paper, the performance of the DBQUS, a standard compliant WiMAX scheduler for integrated EPON-WiMAX network was assessed. Simulation results showed the robustness of the DBQUS scheduler which was able to provide the required QoS under variability of the channel capacity. As the traffic load increases, the bandwidth received by the BE service flow is reduced due to the service provided to classes of service with higher priority. Moreover, the DBQUS furnishes the QoS requirements of different services flows specified in the standard under different EPON service cycles.

Such robustness reinforces the adequacy of the DBQUS scheduler for integrated EPON-WiMAX networks, specially because it does not require any change in the EPON network.

References

[1] C. Cicconetti, L. Lenzini, E. Mingozzi, and C. Eklund, "Quality of service support in ieee 802.16 networks," *Network, IEEE*, vol. 20, pp. 50–55, March-April 2006.

[2] M. Mcgarry, M. Reisslein, and M. Maier, "Ethernet passive optical network architectures and dynamic bandwidth allocation algorithms," *Communications Surveys and Tutorials, IEEE*, vol. 10, pp. 46–60, 2008.

[3] G. Shen, R. Tucker, and C.-J. Chae, "Fixed mobile convergence architectures for broadband access: Integration of epon and wimax," *Communications Magazine, IEEE*, vol. 45, pp. 44–50, August 2007.

[4] M. Dias and N. L. S. da Fonseca, "Performance evaluation of a scheduler for the onu-bs of integrated epon-wimax networks," in *IEEE 3rd Latin-American Conference on Communications*, pp. 1–6, 2011.

[5] I.-S. Hwang, J.-Y. Lee, C.-W. Huang, and Z.-D. Shyu, "Advanced dynamic bandwidth allocation and scheduling scheme for the integrated architecture of epon and wimax," *Mobile Data Management, IEEE International Conference on*, vol. 0, pp. 655–660, 2009.

[6] K. Yang, S. Ou, G. K., and H.-H. Chen, "Convergence of ethernet pon and ieee 802.16 broadband access networks and its qos-aware dynamic bandwidth allocation scheme," *Selected Areas in Communications, IEEE Journal on*, vol. 27, pp. 101–116, February 2009.

[7] Y. Yan, H. Yu, H. Wang, and L. Dittmann, "Integration of epon and wimax networks: uplink scheduler design," No. 1 in 7, SPIE, 2008.

[8] T. Tang, G. Shou, Y. Hu, and Z. Guo, "Performance analysis of bandwidth allocation of convergence of wimax and epon," *Networks Security, Wireless Communications and Trusted Computing, International Conference on*, vol. 1, pp. 662–665, 2009.

[9] Y. Luo, S. Yin, T. Wang, Y. Suemura, S. Nakamura, N. Ansari, and M. Cvijetic, "Qos-aware scheduling over hybrid optical wireless networks," in *Optical Fiber Communication and the National Fiber Optic Engineers Conference, 2007. OFC/NFOEC 2007. Conference on*, pp. 1–7, March 2007.

[10] Alsolami, F. Jaber, Ho, and Pin-Han, "A novel two-level hierarchical scheduling scheme for integrated wimax and epon," *IEEE Communications Surveys and Tutorials*, vol. 3, pp. 46–60, 2009.

[11] G. Kramer, B. Mukherjee, and G. Pesavento, "Ipact: a dynamic protocol for an ethernet pon (epon)," *Communications Magazine, IEEE*, vol. 40, pp. 74–80, Feb 2002.

[12] J. F. Borin and N. L. S. Fonseca, "Uplink scheduler and admission control for the ieee 802.16 standard," *Globecom*, 2009.

[13] J. F. Borin and N. L. S. da Fonseca, "Scheduler for ieee 802.16 networks," *IEEE Communications Letters*, vol. 12, no. 4, pp. 274 – 276, 2008.

[14] J. Farooq and T. Turletti, "An IEEE 802.16 WiMAX Module for the NS-3 Simulator," *Proceedings of the Second International ICST Conference on Simulation Tools and Techniques*, 2009.

[15] 3GPP2 C.S0014-0, "Enhanced Variable Rate Codec (EVRC)."

[16] F. H. Fitzek and M. Reisslein, "Mpeg-4 and h.263 video traces for network performance evaluation," *IEEE Network*, vol. 15, pp. 40–54, Dec 2001.

[17] G. Kramer and B. Mukherjee, "Supporting differentiated classes of service in ethernet passive optical networks," *journal of Optical Networking*, vol. 01, 2002.

Reduced Dimension Policy Iteration for Wireless Network Control via Multiscale Analysis

Marco Levorato*†, Sunil Narang†, Urbashi Mitra† and Antonio Ortega†
∗ Dept. of Electrical Engineering, Stanford University, Stanford, CA 94305 USA
† Dept. of Electrical Engineering, University of Southern California, Los Angeles, USA.
{ }

***Abstract*— A novel framework for the analysis and optimization of wireless networks operations is proposed. The temporal evolution of the state of the network is modeled as the trajectory of the state of a Finite State Machine (FSM). The state space of the FSM and the statistics of state transition are represented as a directed graph. Graph reduction and transform techniques are proposed to reduce the dimension of the graph associated with the FSM and analyze the properties of functions defined on its state space. The proposed methodology is based on the intrinsic multi-dimensional/multi-scale structure of the state space of the FSM and enables the analysis and minimization of cost-to-go functions, *i.e.*, functions measuring the expected long-term cost associated with a control strategy, on coarser versions of the original graph.**

I. Introduction

As wireless communication systems evolve and advance, accurate modeling and thus system optimization becomes more complex and computationally expensive. Heterogeneity of mobile devices and standards further exacerbates the problem. Smart transmission strategies (*e.g.*, [1]–[3]) have been proposed to adapt the operations of wireless terminals to the surrounding networking and natural environment. Increasingly, wireless networks are cyberphysical systems coupling the natural environment with an engineered one. Learning the environment (including the behavior of interfering users) and optimizing the strategy in real-world scenarios is prohibitively demanding in terms of observation time and computational complexity. We propose a novel framework for the analysis and optimization of transmission strategies for wireless networks based on graph wavelet transforms, graph reduction, and sparse approximation.

The methodology presented herein is based on the representation of the Finite State Machine (FSM) modeling the temporal evolution of the network as a multi-dimensional graph. The vertices of the graph are states of the FSM and the edges are allowed state transitions. FSMs have been traditionally used to model the operations of wireless networks, see [4]–[8]. Cost-to-go functions [9] measure the expected long-term cost incurred by the network given a transmission strategy and a cost function defined on the state space of the FSM. These functions can be defined to measure performance metrics of interest (*e.g.*, throughput, packet delivery rate, buffer congestion) and are intimately connected to the behavior of the network and the structure of the stochastic processes determining the trajectory of the network within the state space of the FSM.

Due to the complexity of the operations of the network, the state space of the FSM is extremely large, and the analysis of the behavior of the network is prohibitively complex. Therefore, instead of operating on the original graph, it would be desirable to find and operate on smaller graphs with fewer nodes and a function representing a smooth approximation of the original cost-to-go function. Moreover, such systems need to employ localized operations which could be computed at each node by using data from a small neighborhood of nodes around it. Multi-channel wavelet filterbanks, widely used as a signal processing tool for the sparse representation of signals, possess both these features (i.e. smooth approximations and localized operations). While wavelet transform-based techniques would seem well suited to provide efficient local analysis, a major obstacle to their application to FSM graphs is that unlike images, the nodes connected via links in these graphs are not immediate neighbors. Therefore, standard wavelet transforms which are based on analyzing immediate neighborhoods around each pixel, are not appropriate to analyze these graphs, and so we require graph based wavelet transforms. In [10] we showed that, thanks to the intrinsic structure of the FSM induced by transmission and networking protocols, a concise representation of cost-to-go functions is achieved by projecting these functions onto graph diffusion wavelet [11] domains. A major shortcoming of diffusion wavelets is that they form an over-complete basis, and do not provide an intuitive understanding of the wavelet coefficients obtained in the transform. In this paper, we propose a framework based on the structure of the FSM, which allows the cost-to-go functions to be analyzed like regular multi-dimensional signals, such as images. The framework is based on the critically sampled two-channel wavelet filterbanks presented in [12]–[14]. Specifically, we exploit the multi-dimensional regular structure of the state space of the FSM, to design subsampling (graph reduction) and graph filtering techniques to analyze stochastic processes, tracking the behavior of wireless networks. Our methodology facilitates the reduction of analysis and computational complexity associated with cost-to-go functions and enables the design of practical, adaptive control algorithms for wireless networks. The contributions of the present paper are: 1) the first framework connecting the graphical structure of the stochastic processes modeling wireless network operation to image processing-like analysis tools; 2) design of a graph reduction and filtering technique for these graphical structures based on [12]–[14]; 3) construction

Prof. Mitra's and M. Levorato's work was supported in part by the National Science Foundation (NSF) under Grant CCF-0917343 and by the AFOSR under grant FA9550-12-1-0215. Prof. Ortega's and S. Narang work was partially supported by the NSF under grant CCF-1018977.

of a policy iteration algorithm [9] operating on the reduced graph. We remark the one proposed herein is the first framework providing a methodology for the analysis of wireless networks operations based on graph wavelets.

The rest of the paper is organized as follows. Section II describes the stochastic model of the network and defines the cost-to-go function. The structure of FSMs modeling of wireless networks operations and of the associated graphs is discussed in Section III. Section IV presents the graph subsampling strategy and the wavelet design for the study of wireless networks' operations. Numerical results are presented in Section V to illustrate and assess the performance of the proposed methodology. Section VI concludes the paper.

II. Stochastic Model of the Network and Performance Metrics

The network evolves according to a FSM with state space $\mathcal{S}$. The trajectory of the state of the FSM within $\mathcal{S}$ is modeled as a Markov process $\mathbf{S}{=}\{S(0), S(1), S(2), \ldots\}$, where $S(t){\in}\mathcal{S}$ is the state of the network at time $t{\in}\mathbb{N}^+$. The system is controlled by the sequence $\mathbf{U} = \{U(0), U(1), U(2), \ldots\}$, where $U(t){\in}\mathcal{U}$ is the action selected at time t and $\mathcal{U}$ is the action set.

The transition probabilities of the Markov process are defined as

$$p(s, u, s') = P(S(t+1) = s' | S(t){=}s, U(t) = u), \quad (1)$$

$\forall s, s'{\in}\mathcal{S}$ and $u{\in}\mathcal{U}$, where $P(\cdot)$ denotes the probability of an event. The performance of the network is measured through a cost function $c(s, s')$ that assigns a positive finite cost to the transition from state s to state s' in $\mathcal{S}$ given that action u is selected. The function

$$c(s, u) = \sum_{s' \in \mathcal{S}} p(s, u, s') c(s, u, s'), \quad \forall s{\in}\mathcal{S}, \quad (2)$$

is the average cost from state s conditioned on the action u. The function $c(s, u)$ can be defined to measure performance metrics such as throughput, packet delivery delay and probability [15].

We consider randomized memoryless policies $\mu(s, u)$, mapping every state $s{\in}\mathcal{S}$ to the probability that control $u{\in}\mathcal{U}$ is selected. This class of control policies is shown to be optimal for optimization problems where the objective function and the constraints are time averages of cost functions [16]. We can then define *expected long-term discounted cost* from state s given that action u is used conditioned on the policy μ as

$$V_\mu(s, u) = c(s, u) + \sum_{\tau=1}^{\infty} \sum_{s' \in \mathcal{S}} \gamma^\tau p_\mu^\tau(s, s') c_\mu(s') \quad (3)$$

where $\gamma{\in}(0, 1)$ is the discount factor, $c_\mu(s) = \sum_{u \in \mathcal{U}} c(s, u)\mu(s, u)$ and $p_\mu^\tau(s, s')$ is the τ-step transition probability conditioned on the policy μ. The transition probability $p_\mu^\tau(s, s')$ can be computed recursively as

$$p_\mu^\tau(s, s') = \sum_{s'' \in \mathcal{S}} \sum_{u \in \mathcal{U}} p(s, u, s'')\mu(s, u) p_\mu^{\tau-1}(s'', s'), \quad (4)$$

with $p_\mu^0(s, s'){=}1$.

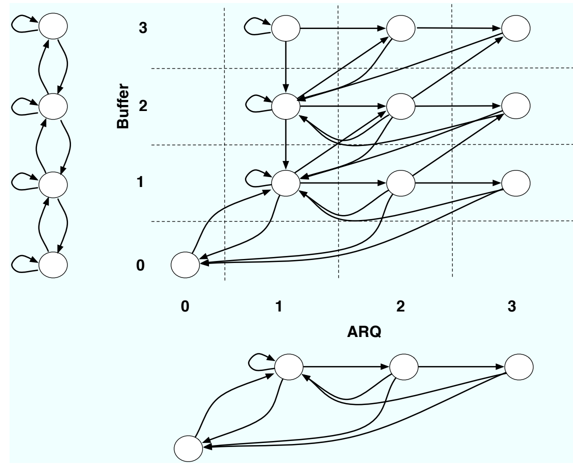

Fig. 1. Graph structure resulting from the composition of sub-chains tracking the number of retransmissions of a packet and the number of packets in the buffer of a wireless node.

The function V_μ is the fixed point solution of the system of equations

$$V_\mu(s, u) = c(s, u) + \gamma \sum_{s' \in \mathcal{S}} p_\mu^1(s, s') V_\mu(s', u), \quad (5)$$

and is generally referred to as the *cost-to-go* function.

The computation, analysis and learning of the cost-to-go function is central in the optimization of transmission strategies in smart and cognitive networks. This class of functions defined on the state space of the network is intimately connected to the structure of the Markov process and is typically optimized via iterative online and offline Dynamic Programming [9]. However, the complexity of the operations of wireless networks limits these approaches to toy scenarios addressing specific aspects of the network (*e.g.*, adaptation to channel variations, channel access).

III. Graphical Structure of the Markov Process

The FSM and the Markov process that determines its trajectory are associated with a directed graph $G = \{\mathbf{V}, \mathbf{E}\}$ where the vertices $\mathbf{V}$ are the states in the state space $\mathcal{S}$ and the edges $\mathbf{E}$ are allowed state-transitions.

As observed in [10], the graph G associated with FSMs modeling wireless networks is the composition of smaller graph structures G_i referred to as *sub-chains*. The sub-chains are small FSMs that track individual counters and variables associated with the behavior of protocols and the evolution of the natural environment. For instance, typical sub-chains track channel state, number of re-transmission of a packet, backoff countdown counter, number of packets in a buffer, *etc.* [4], [15]. Although the transition probabilities from one state to another in $\mathcal{S}$ depend on the whole state description and cannot be expressed as the product of transition probabilities of the sub-chains, the *connectivity structure of the overall graph is the composition of the connectivity structure of the sub-chains*. In fact, if a transition from one state to another in a sub-chain is not allowed, any transition in the complete graph containing that sub-chain transition has probability equal to zero. As a consequence, the connectivity structure of the overall graph inherits key properties of the connectivity structure of the sub-chains.

Interestingly, typical sub-chain constructions for wireless networks can be categorized into a small number of classes [10]. These notable constructions are associated with *regular* and *local* graphs. By regular and local we mean that many states connect to their 1-hop neighbors in a similar fashion and that the number of allowed state transitions is small, respectively.

Fig 1 shows the graph resulting from the composition of a sub-chain modeling the temporal evolution of the number of packets in a buffer of a wireless terminal and a sub-chain modeling the retransmission process of a packet determined by an Automatic Retransmission reQuest (ARQ) protocol. The state space of the FSM is $\mathcal{S}{=}s(0,0)\cup\{s(f,b)\}_{f=1,\dots,F,b=1,\dots,B}$, where $s(f,b)$ denotes the state in which f retransmissions of the packet being served by the terminal have been performed and b packets are stored in the buffer. The parameters B and F are the size of the buffer and the maximum number of retransmissions, respectively. State 0 corresponds to an idle terminal with an empty buffer. The Markov process modeling the temporal evolution of the number of packets in the buffer admits limited increases/decreases due to packet arrival and delivery. Thus, in the associated sub-chain, vertices connect to a limited number of neighbors, that is, vertices associated with a bounded increase/decrease of the number of packets. Although the wireless terminal may implement channel access and transmission strategies such that packet delivery and admittance in the buffer depend on the number of packets in the buffer,[1] the connectivity structure of the sub-chain is generally independent of the current state and, thus, extremely regular. The retransmission process counts the number of transmissions of a packet and resets the counter either if the packet is delivered or the maximum number of retransmission F is reached. Thus, in the associated sub-chain, all states connect to the state corresponding to the next transmission and to the states corresponding to the first transmission of a new packet and the idle state 0. The connectivity structure of the sub-chain associated with the retransmission process is, then, local and regular. The overall graph resulting from the composition of these sub-chains also has a regular and local connectivity structure. As explained in Section IV, regularity and locality of the graph along the sub-chain directions are fundamental for the wavelet construction proposed herein.

IV. Wavelet Analysis

The sub-chain decomposition defines *dimensions* in the state space along which the graph presents regular connectivity structures. The framework proposed herein exploits this decomposition to define sub-sampling strategies and to design graph transform techniques for the reduction of graphs associated with the operations of wireless networks. We then analyze properties of the cost-to-go function and perform iterative strategy optimization on the *coarser* graph to reduce

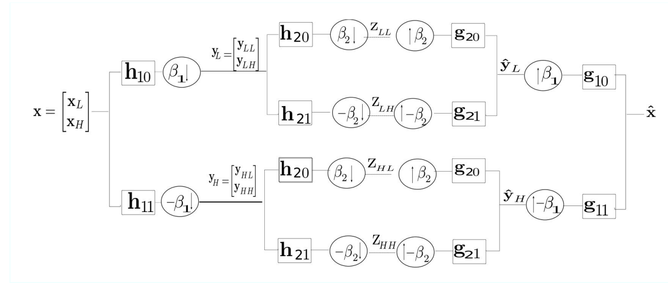

Fig. 2. Graph filterbank operating on two different bipartite sub-graphs.

the dimension of the problem. We will use the retransmission-buffer graph structure described in Section III as exemplar for the design of the proposed wavelet construction and framework. However, the technique can be applied to a wide class of FSMs modeling the operations of wireless networks.

A. Graph-QMF filterbanks

In our recent work [12]–[14], we have designed critically sampled two-channel wavelet filterbanks, called *graph-QMF*, for arbitrary undirected weighted graphs. The filterbanks are implemented as "one-dimensional" two-channel filterbanks on bipartite graphs, and then extended as separable "multi-dimensional" two-channel filterbanks for arbitrary graphs via a novel bipartite subgraph decomposition scheme. The dimensionality refers to the direction of filtering and down-sampling in graphs (detailed discussion in [14]). According to the formulation proposed in this work, a graph G is first decomposed into a set of edge-disjoint bipartite subgraphs $\mathcal{B}_k = (L_k, H_k, E_k)^2$ for $k = 1, 2, ...K$, and then filtering and downsampling operations are carried out in cascade on each bipartite subgraph, as shown in Figure 2. Thus, the bipartite subgraph decomposition provides an interpretation of the graph in terms of "direction" or "dimensions", where a dimension refers to a direction of filtering and downsampling in graphs. The "one-dimensional" filtering operations on each bipartite subgraph $\mathcal{B}_k$ are linear transforms, implemented as polynomials of the normalized graph Laplacian matrix $\mathcal{L}_{\mathbf{k}} = \mathbf{I} - \mathcal{A}_{\mathbf{k}}$, where $\mathcal{A}_k$ is the normalized node-node adjacency matrix. We work with a spectral representation of graphs, in which the eigenvalues of $\mathcal{L}$ are chosen as *graph frequencies* with the corresponding eigenvectors as *Fourier basis*. With this representation, the filters on graphs are first designed as polynomial bandpass kernels in the spectral domain, and then the polynomial coefficients are used to compute the actual filters as matrix polynomials of $\mathcal{L}$. Further, the downsampling in a bipartite graph $\mathcal{B} = (L, H, E)$ is carried out such that the nodes in subset L (or H) store the output of only low-pass (or high-pass) channels. We have shown [12] that, for bipartite graphs, the effect of downsampling followed by upsampling is analogous to well known aliasing, a property which allows us to define the two-channel perfect-reconstruction conditions of the filterbanks in very simple terms.

[1]For instance, backpressure algorithms to stabilize the queue of packets [17].

[2]A bipartite graph $\mathcal{B} = (L, H, E)$ is a graph whose vertices can be divided into two disjoint sets L and H, such that every link connects a vertex in L to one in H.

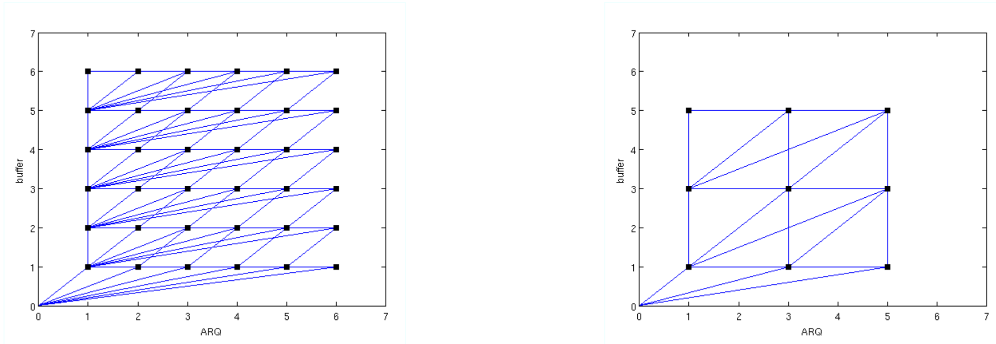

(a) Graph at level 0 (b) Graph after downsampling

Fig. 3. Example network graph with two variables.

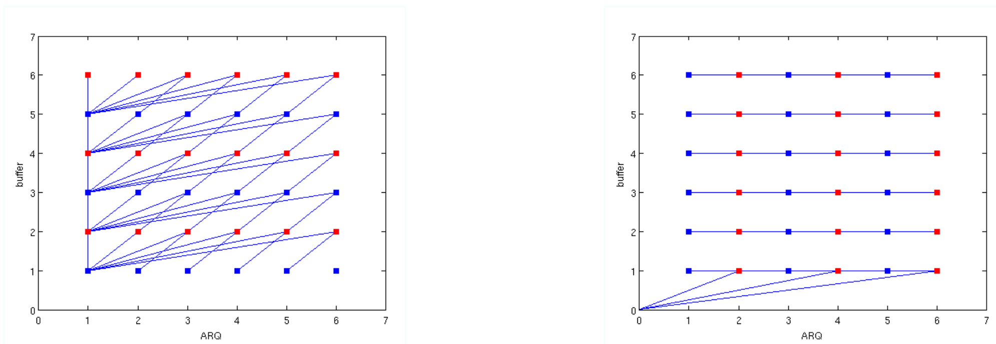

(a) Bipartite subgraph $\mathcal{B}_1$ (b) Bipartite subgraph $\mathcal{B}_2$

Fig. 4. Example of bipartite subgraph decomposition. The color of nodes (red/blue) are bipartitions (L_k, H_k) induced by the bipartite subgraphs.

Subsequently, the filtering and downsampling operations in the "multi-dimensional" implementation are the product of K filtering operations, one on each bipartite subgraph, followed by K downsampling operations. The strategy for decomposition of graph into bipartite subgraphs is non-unique. However, in [14] it is shown that optimal decomposition strategies lead to mutually orthogonal filtering and downsampling operations. We denote the graph transform pair $\{\mathbf{H}_{k0}, \mathbf{H}_{k1}\}$ as the analysis low-pass and analysis high-pass wavelet filters respectively on k^{th} subgraph. Thus, for a "two-dimensional" decomposition, the filterbank provides a 4-*channel decomposition* of the value-functions with channel responses $\mathbf{H}_{2j}\mathbf{H}_{1i}$ for $i, j = 0, 1$, and the output coefficients stored at disjoint nodes $LL = L_2 \cap L_1$, $LH = L_2 \cap H_1$, $HL = H_2 \cap L_1$ and $HH = H_2 \cap H_1$. Compared to other wavelet designs (*e.g.*, [11], [18]), the proposed construction enables the analysis of properties of cost-to-go functions in the wavelet representation. Further, unlike diffusion wavelets [11], used in [10] to accelerate learning, the proposed transforms are critically sampled (i.e., the number of output samples equals to the number of input samples), and do not require a separate dictionary learning algorithm to compute an orthogonal basis. Further, the proposed transforms have a localized spatial spread at each node, and provide an easy interpretation of the basis functions used in the wavelet representation. This implies, that the low-pass transform output can be interpreted as a new function on the downsampled graph, and the proposed two-channel wavelet filterbanks can be recursively applied, enabling a *multi-resolution analysis*. Both analysis and synthesis filters in the graph-QMF filterbank are finite impulse response (FIR) filters, designed using a prototype spectral response, which is a m^{th} order polynomial approximation of the Meyer wavelet like kernel in the continuous interval $[0\ 2]$. Here, m is a parameter of graphQMF design, given which the filters in the graph filterbank can be computed in m iterative steps. Each step requires $\mathcal{O}(|E|)$ operations where $|E|$ are the number of edges in the graph. Since, the graphs in our study are regular graph, $|E|$ scales linearly with the number of nodes N in the graph. Thus, the complexity of implementing graph filterbank in our case is $\mathcal{O}(mN)$.

B. *Implementation on network graphs*

The graph-QMF filterbanks are based on undirected graphs. However, promising results are achieved by techniques, such as those in [10], converting the directed graph structures related to the evolution of FSMs into undirected before applying the transform. Figure 3(a) shows an undirected version of the graph G of Figure 1. Any cost-to-go function on the graph G can be represented as a two-dimensional signal, with variations in ARQ and buffer dimensions as shown in Figure 5. In general, for a network-graph G resulting from the composition of K sub-chains, the corresponding cost-to-go function can be represented as a regular K-dimensional signal. This representation of G can be compared with a two-

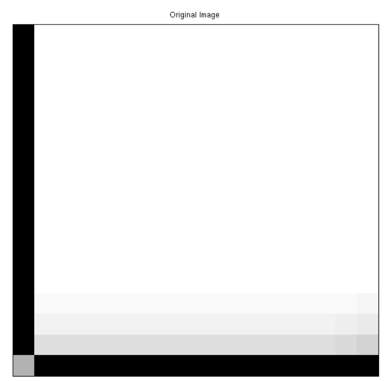

Fig. 5. Two-dimensional image-like representation of value function. The intensity of pixels represents magnitude of value-function (black = 0, white = max).

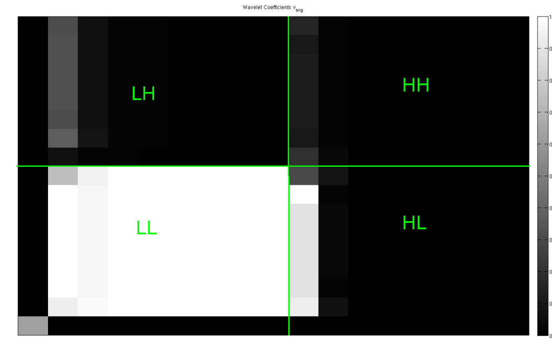

Fig. 6. Graph-QMF wavelet coefficients after one level decomposition of value-function ($m = 24$).

dimensional graph representation of an image [12], with states as pixels and value-functions as pixel-intensities. Note that, the link-structure of these network graphs is quite different from the regular 4 (or 8)-connected (NWSE) link-structure of image-graphs, and hence analysis using standard image wavelet filterbanks is not appropriate in this case. Therefore, we require a graph based wavelet filterbanks.

In order to implement graph-QMF filterbanks, we first decompose G into bipartite subgraphs, and then implement "one-dimensional" graph-QMF filterbanks, one by one on each subgraph. While the bipartite subgraph decompositions of arbitrary graphs require search algorithms, to be computed in an optimal fashion [14], the regular and local structure of network graphs along the subchains, provide a natural decomposition of graph into state-variable (ARQ, buffer, etc.) dimensions. The bipartite subgraph decomposition of graph G is shown in Figure 4. In this decomposition scheme, the bipartite subgraph $\mathcal{B}_1$ consists of *all the links* that connect the states in each row to the states above and below the row, while bipartite subgraph $\mathcal{B}_2$ consists of *remaining links* that connect states in each column to the states in the left and right columns. Thus the filtering operations on $\mathcal{B}_1$ measure variation of value functions in the buffer direction while the filtering operations on $\mathcal{B}_2$ measure variation in the ARQ direction.

Given such a decomposition, a two-dimensional graph-QMF filterbank is applied to the graph. The wavelet coefficients obtained from the first level decomposition of a value-function are shown in Fig. 6. Note that, in Figure 6, the size of output-coefficients is equal to the size of the cost-to-go function (i.e., number of states), and provide a near lossless reconstruction of the original cost-to-go function. Further, the LL channel coefficients, which are now aggregated on the LL-nodes (i.e., nodes sampled in the LL channel), provide a smooth approximation of the cost-to-go function. The other channels (LH,HL and HH) coefficients are mostly sparse, and non-zero coefficients are concentrated in the regions where the magnitude of the cost-to-go function changes. For example, the wavelet coefficients have high-magnitude in the first column in LH subband channel, implying that the cost-to-go function changes significantly from states with $ARQ = 1$ to $ARQ = 2$. Thus, the graph-QMF wavelet filterbanks provide a decomposition of cost-to-go functions similar to standard wavelet filterbanks.

For next level of decomposition, the LL-channel coefficients, are treated as cost-to-go functions on the downsampled, lower-dimension graph. The reconnection strategy of the lower-dimension graph is decided based on the connectivity structure of the original graph. In our proposed strategy, each LL-node $\hat{s}(f,b)$ represents a cluster of states, given as $s(2f,2b)$, $s(2f,2b-1)$, $s(2f-1,2b)$ and $s(2f-1,2b-1)$, in the original graph. The link-weight between two states $\hat{s}(f,b)$ and $\hat{s}(f',d)$ in the downsampled graph is equal to the sum of edge-weights of all connections from the cluster of states represented by $\hat{s}(f,b)$ and $\hat{s}(f',d)$, in the original graph, i.e.,

$$p(\hat{s}(f,b),\hat{s}(f,d))=\sum_{i,j,k,l=-1}^{i,j,k,l=0} p(s(2f-i,2b-j),s(2f-k,2b-l)) \tag{6}$$

The downsampled graph G_1 in the LL-channel, corresponding to the example graph shown in Figure 3(a) is shown in Figure 3(b). A bipartite subgraph decomposition similar to Figure 4 can be applied to downsampled graph G_1, and so on thus leading to a full multi-resolution analysis of cost-to-go functions. The wavelet coefficients after two levels of decomposition are shown in Figure 7.

C. Strategy Optimization and Policy Iteration on Reduced Graphs

The coarse reconstructed function and wavelet coefficients at the different levels can be used to analyze the cost-to-go function and optimize control strategies. The optimal strategy μ minimizes the cost-to-go function in all the states in $\mathcal{S}$.

In policy iteration, the strategy μ is optimized by iteratively generating a sequence of policies μ^k, $k{=}0,\ldots,K$ converging in a finite number of steps K to the optimal policy $\mu^*{=}\mu^K$. At iteration k, the function V^k associated with policy μ^k is computed (policy evaluation step) and then the policy μ^{k+1} is generated (policy improvement step). The policy evaluation step is performed by solving the linear system of equations in Eq. (5). In the policy improvement step μ^{k+1} is

$$\mu^{k+1}(s,u) = \begin{cases} 1 & \text{if} \quad u = \min_{u'\in\mathcal{U}} V^{\mu^k}(s,u') \\ 0 & \text{otherwise.} \end{cases} \tag{7}$$

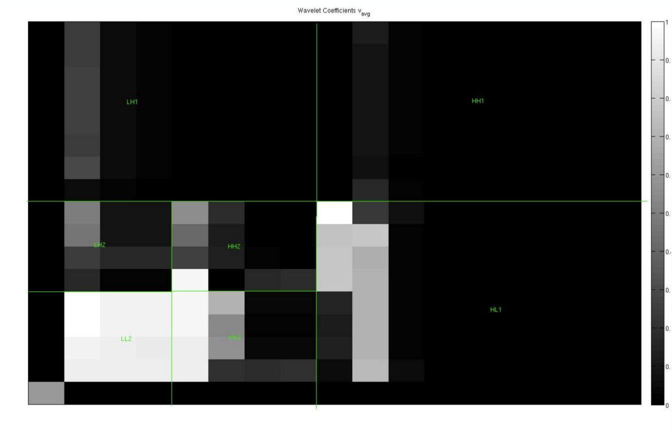

Fig. 7. Graph-QMF wavelet coefficients after 2-levels of decomposition.

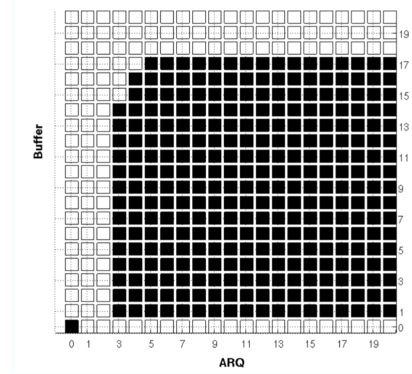

Fig. 8. Optimal policy: black and white squares correspond to states in which the interfering terminal transmits and is idle, respectively. $B{=}F{=}20$.

Iterations end when $\mu^K{=}\mu^{K-1}$. Note that the optimal policy is deterministic. Deterministic policies are optimal for unconstrained optimization problems, whereas in general the optimal policy has a number of *randomizations* equal to the number of constraints [16].

The state space of FSMs modeling the behavior of wireless networks is generally extremely large. Thus, the policy evaluation and improvement step of each iteration are computationally demanding. The technique proposed herein enables a reduction of the dimension of the problem:

- the policy improvement step can be performed on coarser and smoother versions of the cost-to-go function to reduce the number of state-action pairs to be visited. The next policy is generated by comparing a reduced-dimension version of the cost-to-go function associated with the various actions.
- large high-pass coefficients of the wavelet transform identify regions of the state space in which the cost-to-go function changes. States in regions of the state space in which the cost-to-go function remains approximately constant are likely have the same action in the next policy. This allows the reduction of the number of states to be visited.

The graph reduction technique proposed herein enables the computation on cost-to-go functions on coarser versions of the graph preserving the fundamental connectivity structure of the original graph, thus potentially dramatically reducing the complexity of the policy evaluation step. We leave this further development of our framework for future publications.

V. Numerical Results

We use the graph reduction technique to perform policy iteration on the ARQ-buffer example discussed before. We consider the two mutually interfering-link example presented in [2], where an interfering terminal (terminal 2) optimizes its transmission strategy and the interfered terminal (terminal 1) implements ARQ and stores packets in a finite buffer. The action space of the interfering terminal is a binary idleness/transmission space. A detailed description of the transition probabilities and their dependency on the action of the interfering node can be found in [2]. The cost function used to measure the performance of the network is a weighed sum of throughput, packet delivery probability and buffer congestion as defined in [15]. The failure probability of a packet transmitted by a terminal is a function of the set of terminals concurrently transmitting in the same slot. The failure probability of terminal 1 and 2 conditioned on idleness and transmission of the other terminal are ν_1, ν_2, ρ_1 and ρ_2, respectively. The probability that a new packet arrives in the buffer of terminal 1 is denoted by σ. In simulations, the parameters are set as follows: $\sigma{=}0.3$, $\nu_1{=}\nu_2{=}0.1$ and $\rho_1{=}\rho_2{=}0.9$.

A convenient way of representing the cost-to-go function defined on the state-action space is to add the action dimension to the graph. In the considered case the action space is binary, so two replicas of the ARQ-buffer graph structure are needed, where states in the two action planes are linked by transitions dictated by the policy.

We compare the policy produced by policy iteration applied to the full and reduced graph (2-levels of decomposition). Nodes corresponding to one action are used to store the coefficients related to the average of the cost-to-go function

$$V_{\text{avg}}(s) = \frac{1}{2}\left(V(s,1) + V(s,2)\right), \tag{8}$$

whereas nodes corresponding to the other action are used to store coefficients computed for the difference

$$V_{\text{diff}}(s) = \frac{1}{2}\left(V(s,1) - V(s,2)\right). \tag{9}$$

Note that action 1 (idleness) is selected if $V(s,1){\leq}V(s,2)$, that is $V_{\text{diff}}(s){\leq}0$, whereas action 2 (transmission) is selected otherwise. Thus, the coarse version of V_{diff} is used to compute the an approximated policy $\tilde{\mu}^*(s,u)$. The error in the computed policy is measured as

$$\frac{1}{|\mathcal{S}|}\sum_{s\in\mathcal{S}}\sum_{u\in\mathcal{U}}|\mu^*(s,u){-}\tilde{\mu}^*(s,u)|\;|V(s,u){-}\min_{u\in\mathcal{U}}V(s,u)|. \tag{10}$$

This metric corresponds to the average increase of the cost-to-go function due to the approximation.

Fig. 8 and 9 show the optimal policy μ^* and the approximated policy $\tilde{\mu}^*$ computed using the 2-levels decomposition

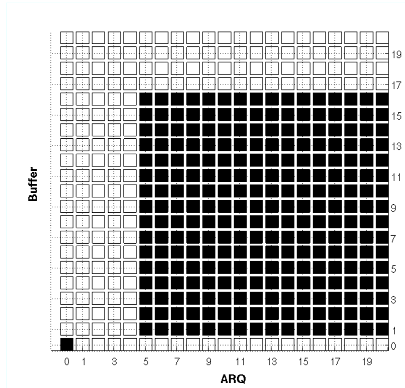

Fig. 9. Policy computed on the reduced graph: black and white squares correspond to states in which the interfering terminal transmits and is idle, respectively. The policy is remapped in the full state space. B=F=20.

of the graph. It can be seen that $\tilde{\mu}^*$ differs from μ^* at the borders of a cluster of states in which transmission is selected. This is due to the loss in resolution resulting from the downsampling process. A possible solution to this issue is to perform adaptive downsampling by detecting edges of action-clusters and keeping high resolution in regions where the cost-to-go function changes. Note that actions tend to cluster in the state space along the connections of the graph due to the smoothness of the cost-to-go function [15].

Fig. 10 shows the policy error as a function of B=F. The error decreases as the size of the graph increases. This is due to the fact that the fraction of states in which the approximated policy differs from the optimal policy decreases. In fact, as observed before errors are more likely to occur on the edges of action-cluster. Since actions cluster in the state space, the size of clusters generally increases and a smaller fraction of erroneous decisions are made. Parameters determining the transition probabilities, and thus the shape and dimension of action-clusters in the graph influence the policy error. As shown in Fig. 10, a larger probability that decoding of packets transmitted by the interfered terminal fails if the interfering terminal is transmitting result in a larger policy error.

VI. Conclusions

A novel framework for the analysis and minimization of cost-to-go functions based on graph reduction and transform techniques was proposed. Properties of cost-to-go functions measuring the performance of the network given a control strategy are analyzed on coarser versions of the graph associated with the FSM modeling the operations of the network. The intrinsic multi-dimensional structure of the FSM defines directions on the graph and allows the construction of graph transform techniques. The framework proposed herein defines a novel methodology for the optimization of the operations of complex networks. Numerical results were presented to show how the proposed technique can be used to optimize the transmission strategy of a wireless terminal.

References

[1] J. Mitola, "Cognitive radio: an integrated agent architecture for software-defined radio," Doctor of Technology, Royal Inst. Technol. (KTH), Stockholm, Sweden, 2000.

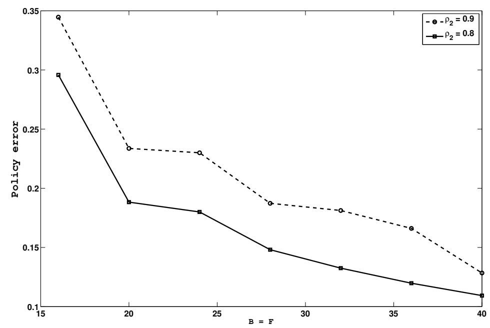

Fig. 10. Error in the policy as a function of B and F.

[2] M. Levorato and U. Mitra and M. Zorzi, "Cognitive interference management in retransmission-based wireless networks," accepted for publication, Trans. on Inform. Theory, 2010. [Online]. Available: http://arxiv.org/abs/1004.0542

[3] R. Zhang and Y. C. Liang, "Exploiting multi-antennas for opportunistic spectrum sharing in cognitive radio networks," *IEEE J. of Sel. Topics in Sig. Proc.*, vol. 2, no. 1, pp. 88–102, 2008.

[4] G. Bianchi, "Performance analysis of the ieee 802.11 distributed coordination function," *IEEE Journal on Selected Areas in Communications*, vol. 18, no. 3, pp. 535–547, 2000.

[5] H. Wu, Y. Peng, K. Long, S. Cheng, and J. Ma, "Performance of reliable transport protocol over IEEE 802.11 wireless LAN: analysis and enhancement," in *proceedings of IEEE INFOCOM*, vol. 2, 2002, pp. 599–607.

[6] M. Zorzi and R. R. Rao, "On the use of renewal theory in the analysis of arq protocols," *IEEE Trans. Commun.*, vol. 44, no. 9, pp. 1077–1081, 1996.

[7] H. Zhai, Y. Kwon, and Y. Fang, "Performance analysis of ieee 802.11 mac protocols in wireless lans," *Wireless Comm. and Mobile Comp.*, vol. 4, no. 8, pp. 917–931, 2004.

[8] M. Dianati, X. Ling, K. Naik, and X. Shen, "A node-cooperative arq scheme for wireless ad hoc networks," *IEEE Trans. Veh. Commun.*, vol. 55, no. 3, pp. 1032–1044, 2006.

[9] D. P. Bertsekas, *Dynamic Programming and Optimal Control*, 2nd ed. Belmont, MA: Athena Scientific, 2001, vol. 2.

[10] M. Levorato, U. Mitra, and A. Goldsmith, "Structure-based learning in wireless networks via sparse approximation," *submitted to the EURASIP Journal on Wireless Communications and Networking, available online: http://www-bcf.usc.edu/∼levorato*, 2012.

[11] R. R. Coifman and M. Maggioni, "Diffusion wavelets," *Applied and Computational Harmonic Analysis*, vol. 21, no. 1, pp. 53 – 94, 2006.

[12] S. Narang and A. Ortega, "Downsampling graphs using spectral theory," in *ICASSP '11.*, May 2011.

[13] S. K. Narang and A. Ortega, "Perfect reconstruction two-channel wavelet filter-banks for graph structured data," *IEEE trans. on Sig. Proc., also avilable in arXiv:1106.3693v3*.

[14] S. Narang and A. Ortega, "Multi-dimensional separable wavelet filter-banks on arbitrary graphs," in *ICASSP '12.*, Mar 2012.

[15] M. Levorato, D. O'Neill, A. Goldsmith, and U. Mitra, "Optimization of arq protocols in interference networks with qos constraints," in *IEEE International Conference on Communications*. IEEE, 2011, pp. 1–6.

[16] K. W. Ross, "Randomized and past-dependent policies for Markov decision processes with multiple constraints," Operations Research, vol. 37, no. 3, pp. 474–477, May-June 1989.

[17] M. J. Neely, E. Modiano, and C. P. Li, "Fairness and optimal stochastic control for heterogeneous networks," in *Proceedings of the IEEE 24th Annual Joint Conference of the IEEE Computer and Communications Societies.*, vol. 3. IEEE, 2005, pp. 1723–1734.

[18] M. Crovella and E. Kolaczyk, "Graph wavelets for spatial traffic analysis," in *IEEE Twenty-Second Annual Joint Conference of the IEEE Computer and Communications (INFOCOM)*, vol. 3, March-April 2003, pp. 1848 – 1857 vol.3.

Benchmarking Message Authentication Code Functions for Mobile Computing

A. M. Rashwan[#1], A-E M. Taha[*2], and H.S. Hassanein[#3]

[#]Telecommunications Research Lab
School of Computing
Queen's University

Electrical Engineering Department
Alfaisal University

***Abstract*— With the increased popularity of both Internet and mobile computing, several security mechanisms, each using various cryptography functions, have been proposed to ensure that future generation Internets will guarantee both authenticity and data integrity. These functions are usually computationally intensive resulting in large communication delays and energy consumption for the power-limited mobile systems. The functions are also implemented in variety of ways with different resource demands, and may run differently depending on platform. Since communications within the next generation Internet are to be secured, it is important for a mobile system to be suited to the function that provide sufficient communication security while maintaining both power-efficiency and delay requirements. This paper benchmarks mobile systems with cryptographic functions used in message authentication. This paper also introduces a metric, namely apparent processing, that makes benchmarking meaningful for mobile systems with multiple processing cores or utilizing hardware-based cryptography. In addition, this paper discusses some of evaluated functions' computational characteristics observed through benchmarking on selected mobile computing architectures.**

Keywords-component; message authentication code; message hashing; next generation Internet security; mobile security;

I. Introduction

Many standards and proposals have been made to ensure the authenticity and data integrity of Internet communications at different levels. Such proposals include IPSec, SSL/TLS, Kerberos, TCP-AO, SCTP-AUTH, to name a few [1]; targeting various services from secured web browsing to protection of intercontinental routing information, and systems from small embedded devices to large mainframes and data centers. Many of those proposals achieve both authenticity and data integrity of transmitted messages with the use of cryptographic functions to generate verification tags, known as *Message Authentication Code* (MAC), to be attached to their corresponding messages.

While the use of cryptography in computing is essential to ensure the security of the information being transmitted through the Internet, it is also known to be computationally challenging. As the importance of security increases with the development of wireless communications and smart portable systems, researchers in security have continued developing, optimizing, and evaluating the performance of various cryptographic approaches. The major focus is finding the approach with strongest security measures and least possible resources demand. As a result, several cryptographic functions had found their ways as software-based and hardware-based solutions to provide message encryption and verification services for various systems and applications. These functions were subject to several research studies evaluating their security and performance, in terms of either the computational power or data throughput.

However, previous studies [2] [3] [4] [5] were evaluating the absolute computational or resource demands of a group of selected functions running on the architecture of study. Only slight considerations were made for how functions behave under dynamically-controlled resource limitations. Cryptographic functions are further attached to other processes, such as communication sessions, and not operated in isolation. Thus, evaluating them for communication purposes should be conducted in a scenario that reflects existence of multiple sessions competing on the existing resources, instead of simply benchmarking for the absolute performance or throughput on the system of study. Especially if the evaluated function is not processed by the same processor where communications are handled – a common setup for many mobile systems [6].

This paper investigates a more comprehensive way to evaluate cryptographic functions that offer MAC services for mobile communications. In this paper, the computational characteristics of some known MAC functions are observed through benchmarking them for communication purposes; under different mobile computing architectures. In doing so, we suggest the use of a new metric, called apparent processing, to facilitate a meaningful comparison between MAC functions. The metric borrows from the notion of apparent parallelism utilized in the context of parallel computing.

The remainder of this paper is organized as follows. Section II refers to some of the related works and describes motivations behind inducting the benchmarking of MAC functions. Section III defines the metric, assumptions, run environments, and used workload for the benchmarking. Evaluation of the benchmarking results is presented in Section IV. Section V lists some additional observed considerations and challenges when benchmarking MAC functions. Finally, conclusion and future directions are mentioned in Section VI.

II. Related Work And Motivation

MAC functions are powered by two types of cryptographic functions: hash or block-cipher [7]. Hash functions, such as MD5, SHA1, and SHA2, are one-way compression algorithms that map variable-length larger messages into shorter fixed-sized strings that vary for different messages. Block-cipher functions, such as AES, TWOFISH, SERPENT, and RC6, are encryption/decryption algorithms designed to work on fixed-sized portions of given messages, called blocks. MACs are generated either by directly hashing combined messages with provided secrets using hash functions, or by hashing message blocks encrypted with provided secrets when using block-cipher-functions.

There are many performance studies of both hash and block-cipher functions in the literature; evaluating different implementations directly and indirectly for various applications [8] [9], architectures [2] [5] [10] [11], and network structures [3] [12]. Those studies were evaluating either the processing power of evaluated functions on certain processing units, or the data throughput that the evaluated functions process.

Today's mobile systems are powered by various single-core and multiple-core processors of different architectures. In addition, several mobile systems are equipped with additional hardware-assisted components to offload computing intensive operations, such as graphics and cryptography, from their main processors, while communications are still maintained by the main processors. Different considerations must be taken into account when benchmarking MAC functions for network communications. These considerations include:

- **Cores Involved.** The future generation Internet protocols, and the future production operating systems in response, will have message authentication as a standard feature. Execution of MAC functions might be locked on certain processor cores so those functions do not render the system unusable in case of high load. Previously conducted performance studies usually focused on the processor power consumed by an evaluated function, without taking into consideration how many cores are utilized by that function.
- **Extra-Processor Computation.** There are implementations of MAC functions that execute outside the main processor (e.g. an external cryptographic processor), yet the main processor still responsible for handling the communication session utilizing the MAC function. Evaluating the processing power on either the main processor or the external processor alone might not be sufficient to indicate the effective performance of that communication session.
- **Implementation Heterogeneity.** A MAC function can have different implementations under same computing architectures, for example, single- threaded and multi-threaded implementations. The determination of superior implementation will be subject preliminary to how the processor will handle them, and how the operating system will schedule their execution. Other factors such as I/O and bus delays may also contribute to the determination.
- **Workload Concurrency.** Previous studies did not consider the use of concurrent workloads (for example, to simulate multiple connections) for their evaluations. With concurrent workloads, effects of scheduling, memory and I/O demands can be reflected on the processing time, giving more realistic performance determination (such as computing the system' capacity in term of number of concurrent connections).

It becomes obvious that there are substantial considerations to be made beyond power or throughput. The objective of this work is to realize an environment to characterize the effect of these considerations.

III. BENCHMARKING SETUP

In order to successfully evaluate the MAC functions for communication purposes within mobile systems, it is important to have a benchmarking setup that effectively describes the true nature of both mobile environments and communications. To achieve this, the benchmarking setup should incorporate the use of mobile production systems, and production operating systems configured for everyday usage. For communications, the setup should be simulate concurrent processing of message authentication as it happens with real communication sessions, and to operate on realistic message lengths that are supported by major mobile communication protocols.

In this paper, the benchmarking setup was designed to fulfill the mentioned objectives. Real architectures from three major known brands in mobile computing were evaluated. A customizable distribution of Linux operating system, which its kernel is powering many of today's mobile systems, is used. The workload was implemented to apply message authentication processing in simulated communication mode, while controlling some operational factors such as cores involved, number of concurrent sessions, and session duration. The workflow was also designed to ensure that the both workloads and their parameters were suitable to apply on studied systems for accurate evaluations. The benchmark metrics were selected to observe computational characteristics of studied systems in both simple and comprehensive ways.

The following elaborates on the details of the benchmarking setup.

A. *Benchmark Environment*

The environment is designed in a manner that ensures that the operating system has minimum influence on obtained results, all benchmarking experiments were conducted under the same OS (Ubuntu Linux 10.04LTS). The chosen operating system, which is running in Gnome desktop mode, uses "Completely Fair" scheduler for scheduling its processes.

Benchmarked architectures were TI DM3730 ARM Cortex A8, Intel Core I3 M350, AMD Opteron 2354, Mobile Intel Pentium 4 3.0GHz. While Opteron is not build for mobile systems, it was included in the benchmark since it was the available AMD architecture at the time of the study, as it shares similar features with its mobile counterpart (Phenom) such as *Cool'n'Quiet*™ speed-stepping (which is a mobile-based feature that reduces processor clock frequency to save energy or reduce operating temperature).

B. *Workload and Workflow*

A multi-threaded benchmarking application is written to evaluate selected MAC functions. The application uses multithreading approach to create workload instances in order to minimize the effect of memory switching on the measurements accuracy. The application was also equipped with a method for binding the execution of the workload instances into certain predefined cores in order to study the effect of limiting the number of available processor cores on the performance of the workload.

The benchmarking workload procedure is illustrated in Figs. 1 and 2. Since typical communication sessions usually runs concurrently with different durations and message lengths, the workload was implemented to simulate such conditions;

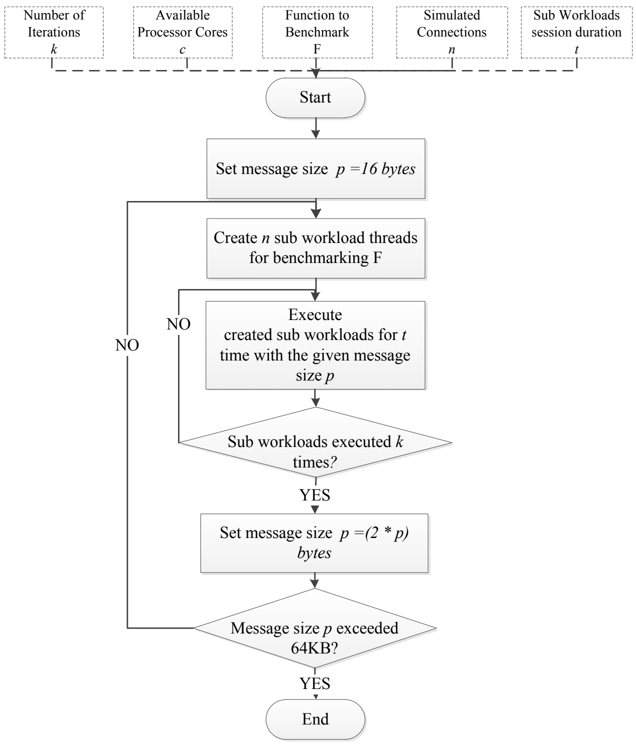

Fig. 1. Benchmark workload procedure

with assumptions of fixed selection of evaluated function and fixed session duration per run to simplify the evaluation. In addition, workload executes the message authentication process same as with a typical production message authentication session. Under each studied architecture, the workload was applied with no other foreground applications running except for the Gnome desktop environment in order to reduce the effect on the measurement accuracy. The workload creates *n* sub workload threads to simulate existence of *n* connections transmitting messages ranging from 16 bytes to 64 kilobytes (the maximum length supported by the IP protocol). For each sub workload, there are *n*-1 background sub workloads representing *n*-1 background connections. In sub workloads, measurements are taken using both the processor clock and the system's wall clock. The period of taking measurements is defined by interval from t_1 to t_2, where t_1 and t_2 are predefined time values between 0 and the execution time t, with $t_2 > t_1$.

Fig. 3 describes the benchmarking workflow procedure. This procedure is essential to ensure workloads being applied to suit benchmarked systems, and measurements obtained are accurate and informative. First, a benchmark scenario is defined to include the number of connections, the function to evaluate, and the processor cores to utilize. Through the process, obtained measurements are analyzed and validated. For example, the accuracy can be affected by resources overutilization, insufficient session duration for reaching the steady state, or inappropriate measurement period. In this case, their corresponding parameters, which are the number of connections *n*, the session duration *t*, and the measurement period $[t_1,t_2]$ will be adjusted accordingly for the next workload.

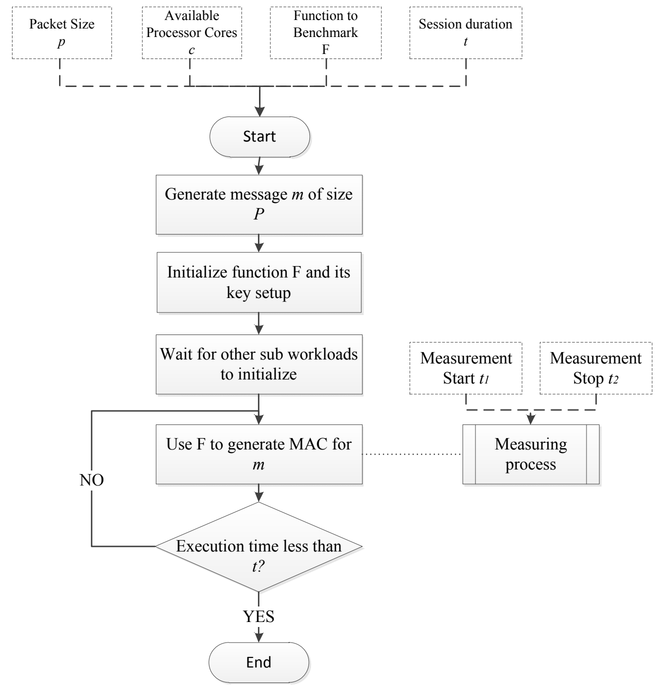

Fig. 2. Benchmark sub workload procedure

C. Evaluated MAC functions

1) Hashed-based MAC (HMAC) [13]: a hash based algorithm, which is being used by various popular Internet protocols (e.g IPSec and TLS [1] [14]) to offer message authentication service during communication sessions Evaluated hash functions under this group are MD5, SHA1, SHA2-256 (simply SHA256) and SHA2-512 (simply SHA512).

2) One-key MAC One (OMAC1): also known as CMAC; a block-cihper based algorithm that was introduced to resolve security flaw of it predecessor, CBC-MAC, when generating MACs for variable-length messages [15]. In 2005, NIST recommended the using of OMAC1 for operating a block-cipher based authentication [16]. Evaluated block-cipher functions under this group are RIJNDAEL, TWOFISH, SERPENT, and RC6, which. were the finalist candidates in *Advanced Encryption Standard* (AES) selection process with Rijndael becoming the official AES [2].

3) VMAC: a block-cipher based algorithm designed to offer high-performance message authentication service [17]. Optimized for 64-bit computing architectures, VMAC utilizes block cipher functions via a "universal hashing" algorithm and secret key to generate MACs for a given message. Evaluated

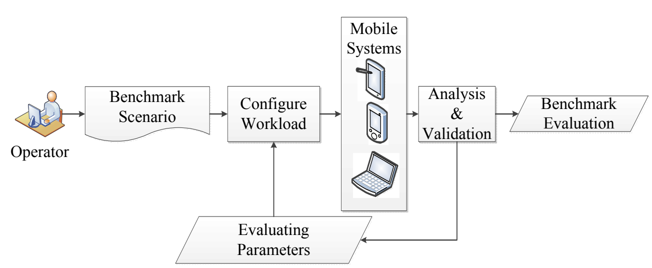

Fig. 3. Benchmark workflow procedure

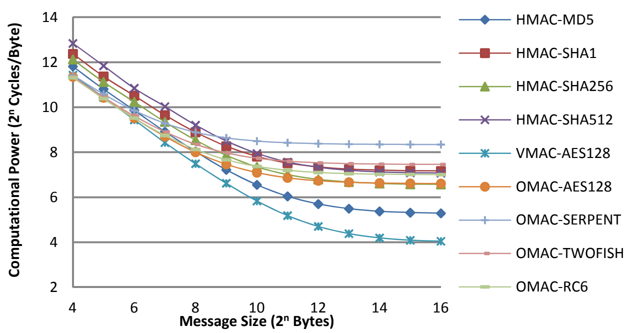

Fig. 4. Absolute Processing Power vs Message Size for different MAC functions under AMD Opteron 2354 @ 1.1GHz with all cores utilized (hardware-assisted compilation of CryptoPP)

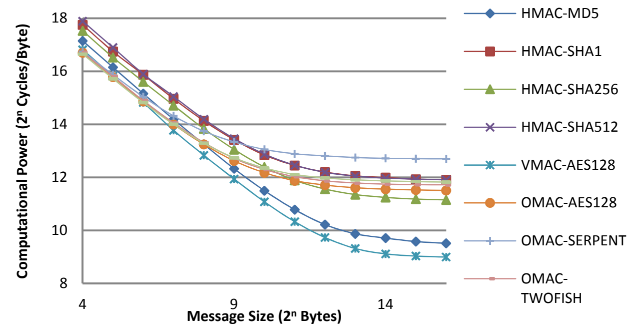

Fig. 5. Absolute Processing Power vs Message Size for different MAC functions under Mobile Intel P4 @ 3.0GHz with hyper-threading disabled (hardware-assisted compilation of CryptoPP)

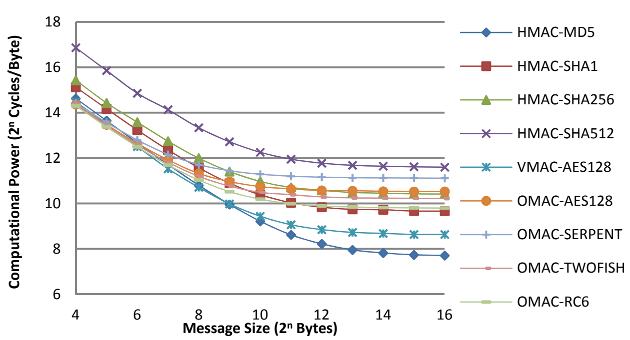

Fig. 6. Absolute Processing Power vs Message Size for different MAC functions under Mobile Intel Core I3 M350 @ 2.26GHz with all cores utilized (software-only compilation of CryptoPP)

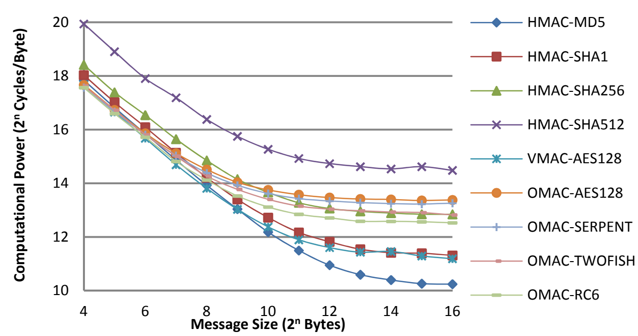

Fig. 7. Absolute Processing Power vs Message Size for different MAC functions under TI DM3730 ARM Cortex A8 @ 1GHz (software-only compilation of CryptoPP)

block-cipher function under this group is AES, which is the only implemetation avaliable for VMAC at the time of study.

D. Cryptograhic Library Used in Benchmarking

A well-known cryptographic library called CryptoPP 5.6.1 is used for this study. This selection is motivated by its popularity among academia for studying cryptographic performance and cryptanalysis [3]. It is also open-source and has cross-platform compatibility, making it suitable to run under various operating systems and computer architectures. The library further has both hardware-assisted and software-only implementations for some functions such as AES (using x86 AES-NI extension) and SHA-256/512 (Using x86 SSE-2 extension); making it a good option to test the effect of different implementations under same hardware. More significantly, the library has its own benchmarking tool that can be used as a validation tool for our benchmarking results.

E. Metrics

Cryptographic functions are known to be computationally demanding, but many of them do not pose high memory and I/O demands; making the processing power the only reasonable evaluation metric. In this paper, two types processing power metrics are considered. The first type presents the choice of most previous studies for evaluating cryptographic functions. While the second type is being introduced in this paper to show the effective performance on mobile systems through evaluating cryptographic functions at external or several processing units. For both types, the less value they have the better performance they indicate.

1) *Absolute Processing Power (presented in cycles/byte):* the number of processor cycles that a MAC function spent on main processor coding one byte of date. This metric is obtained directly from the main processor clock.

2) *Apparent Processing Power (presented in cycles/byte):* the wall clock time, calculated as the number of processor cycles, that a MAC function spent coding one byte of data, as if the function is virtually being executed squentially by the main processor. This metric is introduced for evaluating both multiple-core and hardward-assited systems (adopted from *apparent parallism* defined in [18] for symetric mutilple processor systems).

F. Measuring Assumptions

The following assumptions were made in evaluating the performance of the different MAC functions.

- Only the processing power is measured. Memory usage and I/O demands are not included in this study. However, the apparent processing power should reflect the memory and I/O demands since both memory transfers and I/O waits take time.
- Only the time for generating MACs is measured. Key setup time is considered in this study.
- Measuring overhead is taken into consideration when setting up the workload to minimize its effect on measurement accuracy.

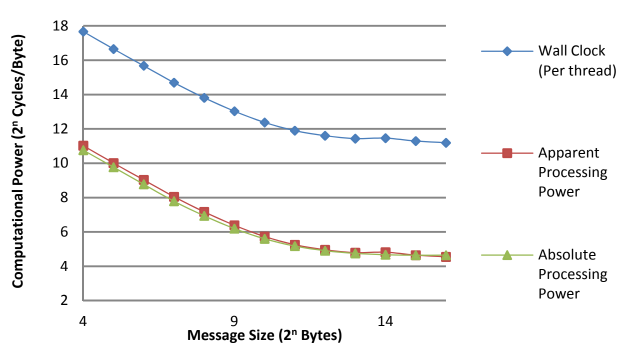

Fig. 8. Wall Clock Cycles,Absolute Processing Power, and Apparent Processing Power of VMAC-AES128 per thread when applying 100-thread workload on TI DM3730 ARM Cortex A8 @ 1GHz

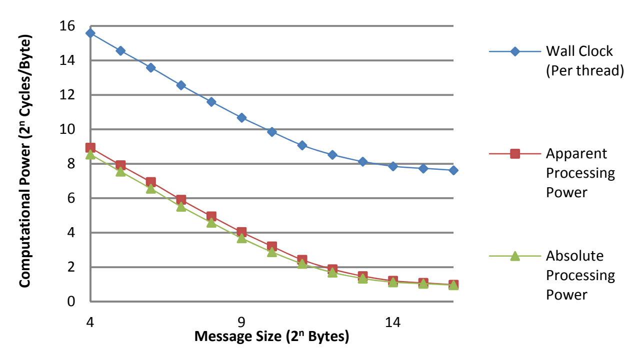

Fig. 9. Wall Clock Cycles,Absolute Processing Power, and Apparent Processing Power of VMAC-AES128 per thread when applying 100-thread workload on one core of Intel Core I3 M350 @ 2.26GHz

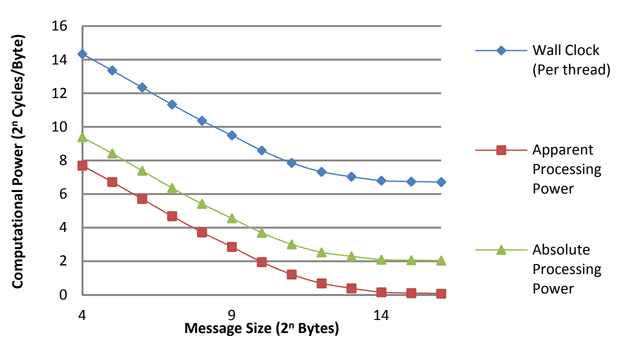

Fig. 10. Wall Clock Cycles,Absolute Processing Power, and Apparent Processing Power of VMAC-AES128 per thread when applying 100-thread workload on both cores of Intel Core I3 M350 @ 2.26GHz

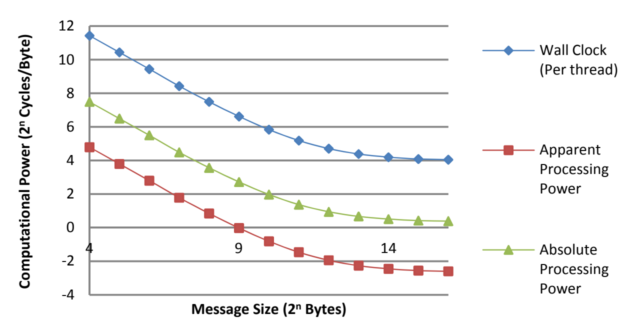

Fig. 11. Wall Clock Cycles,Absolute Processing Power, and Apparent Processing Power of VMAC-AES128 per thread when applying 100-thread workload on all eight cores of AMD Opteron 2354 @ 1.1GHz

- Effect of mobility features, such as speed stepping and thermal protection, on processing delays is not considered in this study.

IV. RESULTS

A. Behaviour of Different MAC generating functions under Different Architectures

Figs. 4, 5, 6 and 7 show the absolute processing power for the evaluated functions under different architectures, and with 100 simultaneous threads per workload.

1) General computational trend for achitectures using the same function implementation: the computational trend, using the same compilation for CryptoPP library, is almost the same across evaluated architectures. The slight differences in performance between different architectures running the same compilations are due to how different processors handle and optimize execution of programs.

2) Computational trend verses message size: it is obvious that the computational trend changes with message sizes under different architectures. Thus, systems and services can optimize the selection of the best performing function based on the size of the transmitted message; provided that other factors such as security stength and key setup time are also taken into consideration.

3) Effect of a function's implementation on computational trend: In the hardware-assisted compilation of CryptoPP, as shown in Figs. 4 and 5, functions such as AES and SHA take advantage of speed boosting. While in Figs. 6 and 7 both AES and SHA lost their advantage, and thus the computational trend has changed with HMAC-MD5 being the fastest processing 64 kilobyte messages, and HMAC-SHA512 being the slowest (as opposed to VMAC-AES128 for fastest and OMAC-SERPENT for slowest in the hardware-assisted compilation).

B. Effect of the number of utilized processor cores

1) Single-core verses multiple-cores architectures: Figs. 8, 9, and 10 show the absolute and the apparent processing power when running a 100 connections VMAC-AES128 workload. For single-core architectures, the apparent processing power should mirror the absolute one, or be slightly higher due to resources demand and measurement overheads. For multiple-core architectures, such as in Figs. 10 and 11, the apparent processing power reflects the effect of parallelism on the performance. As expected, the apparent performance is correlated to the number of cores utilized within the architecture, with additional cores translated to better apparent performance.

2) Utilizing single-core verses multiple-cores: While the apparent performance improved in Fig. 10 (compared to Fig. 9) due to the parallelism effect, the absoluste performance is dropped. One explanation is because the contention between the workload and the operating system, causing the latter to preempt execution of the workload more frequenty. In addition, with the increase of the number of cores, the overhead caused by thread migration between cores might increase as well.

V. Observed Challenges

We note some challenges that were observed through conducting the benchmarking experimenting and workflow procedures. These challenges affect the accuracy of measuring both absolute and apparent processing powers, or in some cases, render them useless as evaluation metrics.

A. Multi-threaded processor architectures

Several computing architectures support execution of two or more threads per core (known as multi-threading cores). Operating systems usually treat each thread as a separate logical core, with no possibility of differentiating it from a physical core. Thus evaluating multi-core systems through limiting available cores can represent a challenge, especially if their main processors have three or more physical cores.

B. MAC function offloading outside the main processor

Some systems might offload MAC functions outside their main processor. Examples of places where MAC functions are offloaded into include *General Purpose Graphic Processing Unit* (GPGPU) and cryptographic processing units. While the performance can be evaluated from the offload unit; it is important not to ignore the main processor in the evaluation since it is still handling communications secured by the offloaded MAC function. In such cases, it will be more logical to benchmark for the apparent processing performance, as if the main processor is executing the functions, although, it will not point to the absolute performance of the evaluated MAC function at the offload unit.

C. Systems with no synchronized clock accross all of its processors or cores

In a multiple processors/cores system, a thread can jump from one processor/core to another. If such a system does not maintain a synchronized clock across all the processors/cores, it is not possible to get the absolute performance for the evaluated MAC function. It will still possible, however, to benchmark for the apparent performance. An estimate for absolute performance can then be made knowing the system's parallelism factor.

D. Operating System Scheduling

It is important to be aware of the scheduling algorithm used by the evaluated operating system. Some operating systems might schedule sub workloads unevenly, which will be mainly reflected in the measured apparent performance. For example, least scheduled threads will have higher apparent processing power than the most scheduled threads of same workload.

VI. Conclusions

Message Authentication Codes (MAC) functions with similar implementations perform with nearly similar computational trends regardless of the computing architecture or its number of cores, the trend depends on the message size. This finding is elemental in selecting the MAC function based on message size, delay, energy, and security requirements. It should also be noted that utilizing all processing cores within a system increases the absolute processing power of MAC functions due to resource contention with the operating system and to overhead of process switching between cores. Systems may therefore employ methods to allocate the number of cores in a manner that optimizes both absolute and apparent processing performance.

The use of the apparent processing power metric for benchmarking seems highly useful when evaluating MAC functions in systems with multiple processors/cores, systems with multi-threaded cores, and systems with offload cryptographic processing units. While the apparent processing performance does not always reflect the absolute performance of the evaluated MAC function, it can be considered as an effective performance metric for communication purposes. However, more investigations are required for finding a feasible relation between the apparent performance and some other factors, such as the used task scheduling and the physical resource requirements of the evaluated MAC function.

Acknowledgment

This research is funded by a grant from Natural Sciences and Engineering Research Council of Canada (NSERC).

References

[1] Internet Official Protocol Standards. RFC 5000, IETF, May 2008, http://www.ietf.org/rfc/rfc5000.txt.

[2] B. Schneier and D. Whiting, "A performance comparison of the five AES finalists," , 2001, p. the 3rd AES Conference (AES3).

[3] Y. W. Law, J. Doumen, and P. Hartel, "Survey and Benchmark of Block Ciphers for Wireless Sensor Networks," *ACM Transactions on Sensor Networks (TOSN)*, vol. 2, pp. 65-93, February 2006.

[4] D. S. Abd Elminaam, H. M. Abdual Kader, and M. M. Hadhoud, "Evaluating The Performance of Symmetric Encryption Algorithms," *International Journal of Network Security*, vol. 10, no. 3, pp. 216–222, 2010.

[5] O. Hyncica, P. Kucera, P. Honzik, and P. Fiedler, "Performance evaluation of symmetric cryptography in embedded systems," in *IEEE 6th International Conference on Intelligent Data Acquisition and Advanced Computing Systems (IDAACS)*, 2011, pp. 277-282.

[6] R. Anderson, M. Bond, J. Clulow, and S. Skorobogatov, "Cryptographic Processors - A Survey," *Proceedings of the IEEE*, vol. 94, no. 2, pp. 357-369, Feb. 2006.

[7] C. Paar, J. Pelzl, and B. Preneel, *Understanding Cryptography: A Textbook for Students and Practitioners*.: Springer, 2010.

[8] M. Sokol, S. Gajewski, M. Gajewska, and L. Staszkiewicz, "Security and Performance Analysis of IPsec-based VPNs in RSMAD," in *The First International Conference on Advanced Communications and Computation (INFOCOMP'11)*, 2011, pp. 70-74.

[9] C. Shen, E. M. Nahum, H. Schulzrinne, and C. Wright, "The impact of TLS on SIP server performance," in *IPTComm'10*, 2010, pp. 59-70.

[10] D. J. Bernstein and P. Schwabe., "New AES software speed records," *INDOCRYPT*, vol. 5365 of LNCS, pp. 322-336, 2008.

[11] D.A. Osvik, J.W. Bos, D. Stefan, and D. Canright, "Fast software AES encryption," *Fast Software Encryption (FSE)*, vol. 6147 of LNCS, pp. 75–93, 2010.

[12] J. Kaps and B. Sunar, "Energy Comparison of AES and SHA-1 for Ubiquitous Computing," in *Embedded and Ubiquitous Computing*, 2006, pp. 372-381.

[13] H. Krawczyk, M. Bellare, and R. Canetti, HMAC: Keyed-Hashing for Message Authentication. RFC 2104, IETF, Feb. 1997, http://www.ietf.org/rfc/rfc2104.txt.

[14] T. Dierks and E. Rescorla, The Transport Layer Security (TLS) Protocol Version 1.2, 2008, http://www.ietf.org/rfc/rfc5246.txt.

[15] Kaoru Kurosawa Tetsu Iwata, "OMAC: One-Key CBC MAC," *Fast Software Encryption (FSE)*, pp. 129-153, 2003.

[16] M. Dworkin, Recommendation for Block Cipher Modes of Operation: The CMAC Mode for Authentication, May 2005, NIST Special Publication 800-38B.

[17] T. Krovetz, "Message authentication on 64-bit architectures," in *13th international conference on Selected areas in cryptography* , 2006, pp. 327-341.

[18] Eli Biham, *Fast software encryption: 4th International Workshop, FSE '97*.: Springer, 1997.